A Study of Energy Savings Potential of Reflective Roof Coatings in U.S. Climate Zones

by

Ajay Kumar Sharma

A Thesis Presented in Partial Fulfillment
of the Requirements for the Degree
Master of Science

Approved April 2024 by the
Graduate Supervisory Committee:

Patrick Phelan, Chair
Narayanan Neithalath
Ryan Milcarek

ARIZONA STATE UNIVERSITY

May 2024

ABSTRACT

This study investigates the energy saving potential of high albedo roof coatings which are designed to reflect a large proportion of solar radiation compared to traditional roofing materials. Using EnergyPlus simulations, the efficacy of silicone, acrylic, and aluminum roof coatings is assessed across two prototype commercial buildings—a standalone retail (2,294 m^2 or 24,692 ft^2) and a strip-mall (2,090 m^2 or 22,500 ft^2)—located in four cities: Phoenix, Houston, Los Angeles, and Miami. The performance of reflective coatings was compared with respect to a black roof having a solar reflectance of 5% and a thermal emittance of 90%. A sensitivity analysis was done to assess the impact of solar reflectance and thermal emittance on the ability of roof coatings to reduce surface temperatures, a key factor behind energy savings. This factor plays a crucial role in all three heat transfer mechanisms: conduction, convection, and radiation. The rooftop surface temperature exhibits considerable variation depending on the solar reflectance and thermal emittance attributes of the roof. A contour plot between these properties reveals that high values of both result in reduced cooling needs and a heating penalty which is insignificant when compared with cooling savings for cooling-dominant climates like Phoenix where the cooling demand significantly outweighs the heating demand, yielding significant energy savings. Furthermore, the study also investigates the effects of reflective coatings on buildings that have photovoltaic solar panels installed on them. This includes exploring their impact on building HVAC loads, as well as the performance improvement due to the reduced temperatures beneath them.

DEDICATION

I dedicate my thesis to my grandparents, parents and my sister, whose unwavering support and guidance have been the foundation of my journey. Their love, encouragement, and belief in me have been the driving force behind my achievements.

ACKNOWLEDGMENTS

I would like to express my heartfelt gratitude to my advisor, Dr. Patrick Phelan, and Dr. Narayanan Neithalath for their unwavering guidance and support throughout this journey. My association with Dr. Patrick Phelan dates back to the beginning of my academic journey at Arizona State University (ASU). Under his mentorship, I gained a wealth of knowledge, particularly through his courses on Refrigeration and Air Conditioning and Energy Efficiency. Working with him at the Industrial Assessment Center (IAC) at ASU, has been a valuable experience that I believe will continue to benefit me in my entire professional career. A significant portion of my master's journey is indebted to his guidance and expertise. Dr. Narayanan's practical way of approaching problems has been very beneficial along with his friendly and easy-to-talk to nature.

I would also like to extend my sincere thanks to Carlisle Weatherproofing Technologies for supporting this work financially. I am particularly grateful to Divya Chopra, Zhiyong Zhu and John Dobson for giving my work thoughtful direction and providing valuable feedback throughout the duration of this work.

Lastly, all of this wouldn't have been possible without Dr. Ryan Milcarek who helped me get involved in IAC that opened additional opportunities for me. He is a great professor, and I am deeply appreciative of the knowledge and guidance gained during my initial semester and at IAC.

TABLE OF CONTENTS

LIST OF TABLES

LIST OF FIGURES

Figure Page

LIST OF SYMBOLS/ABBREVIATIONS

Symbols

A_{pv}	Area of the PV Module (m^2)
E_{elec}	Electrical Energy Output from the Panel (W)
F_{fs}, F_{fr}, F_{bs}, F_{br}	View Factors Between Front Surface-Sky, Front Surface-Roof, Back Surface-Sky, Back Surface-Roof Respectively
h_{conv}	Convection Heat Transfer Coefficient ($W\ m^{-2}\ K^{-1}$)
I_s	Incident Solar Irradiation on the PV ($W\ m^{-2}$)
$Q_{conv,\ pv}$	Heat Dissipated to the Surrounding Air in Form of Convection (W)
$Q_{LW\ rad,\ pv}$	Heat Loss in the Form Long Wave Radiations (W)
Q_{solar}	Solar Energy Absorbed by the Solar Panel (W)
T_{air}	Temperature of Ambient Air (ºC)
T_{dp}	Dewpoint Temperature of Ambient Air (ºC)
T_{pv}	Temperature of PV Module (ºC)
T_{ref}	Reference Temperature, 25ºC
T_{roof}	Temperature of Roof Surface (ºC)
T_{sky}	Temperature of Sky (ºC)
w_{speed}	Wind Speed ($m\ s^{-1}$)
α	Solar Absorptance of PV Cell
β_{ref}	Temperature Coefficient of PV Module
ϵ_b	Emissivity of the Back Surface of PV
ϵ_f	Emissivity of the Front Surface of PV

ϵ_{sky}	Emissivity of Sky
$\eta_{T_{ref}}$	Efficiency at reference temperature of 25ºC and an irradiance of 1000 W m^{-2}
σ	Stefan-Boltzmann constant
τ	Transmissivity of PV glass
θ	Tilt angle of Panel (degree)

Abbreviations

AF	Area Fraction of PV
ASHRAE	American Society of Heating, Refrigerating and Air-Conditioning Engineers
Btu	British Thermal Unit
DOE	Department of Energy
HVAC	Heating, Ventilation and Air Conditioning
IECC	International Energy Conservation Code
NOCT	Nominal Operating Cell Temperature
NREL	National Renewable Energy Laboratory
PV	Photovoltaic
SR	Solar Reflectance
SRI	Solar Reflectance Index
TE	Thermal Emittance
TMY	Typical Meteorological Year
UHI	Urban Heat Island

CHAPTER 1

Introduction

1.1 Urban Heat Island

Presently, around 56% of the global population, equivalent to 4.4 billion individuals, resides in urban areas and projections indicate that this trend will persist, and by 2050, the urban population is anticipated to surpass twice its current size [1].

As shown in Figure 1-1, the world's urban population has consistently risen over the last six decades. It has increased from around 34% in 1960 to over 55% in 2022. Figure 1-2 illustrates the division of urban population based on the population [2].

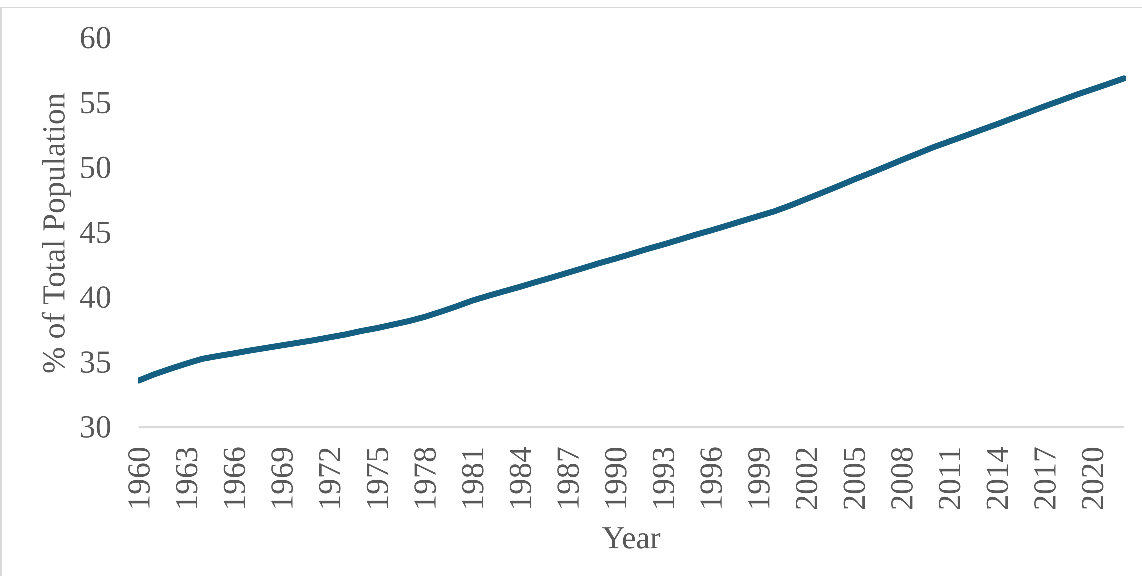

Figure 1-1: Urban Population as Percentage of the Total Population from 1960 to 2022[2]

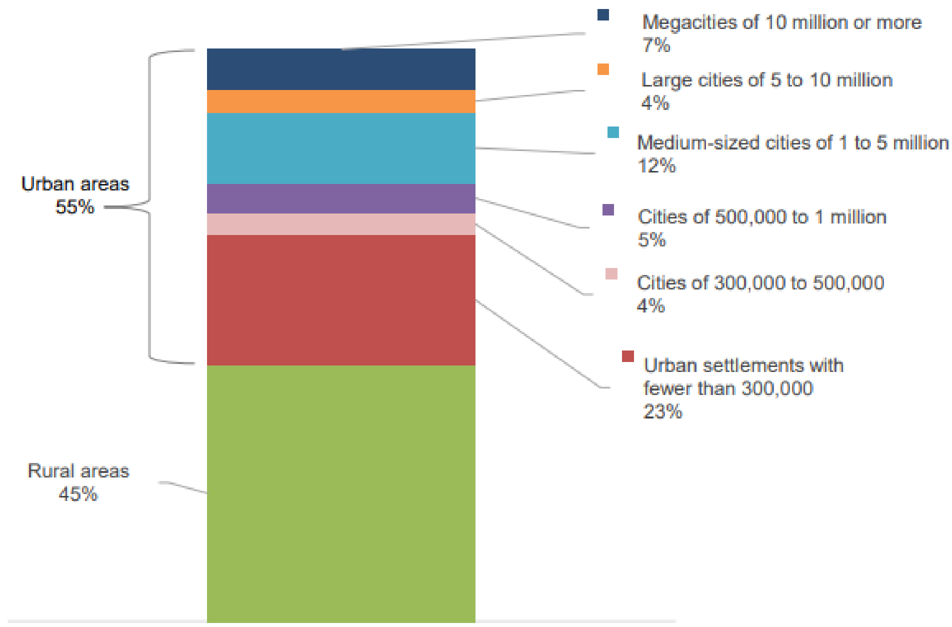

Figure 1-2: Population of the World by Area of Residence and Size Class of Urban Settlement, 2018

This increasing urban population gives rise to a phenomenon known as Urban Heat Island (UHI). Urban Heat Island is characterized by elevated temperatures in urban areas compared to their surrounding rural areas. The primary contributors to the UHI include lower wind speed caused by urban roughness, the entrapment of long-wave radiation within the urban canopy during nighttime, the thermal characteristics of building materials, the scarcity of vegetation etc. [3] In response to the UHI effect, researchers are exploring various mitigation strategies. Among these, the application of reflective coatings on building roofs has gained attention in the last two decades. On a hot summer afternoon, low-reflectance surfaces roofs that absorb a huge amount of heat can have a temperature difference of up to 32.2°C (90°F) compared to the surrounding air [4]. The use of high-reflectance surfaces in urban areas is a cost-effective approach to reduce these high temperatures in summer months.

1.2 Literature review

In hot-dry, warm, humid, and composite climatic zones, roofs play a significant role, contributing approximately 50 to 60% of the total cooling load for buildings. The roof, being a prominent part of the building envelope, is directly exposed to solar radiation, making it a primary contributor to the overall cooling load in the buildings [5]. One of the earliest studies examining the climatic effects of reflective surfaces simulated the impact of albedo modification in Los Angeles, USA. The results indicated that an increase in albedo by 0.14 resulted in decrease in ambient temperatures by at least 0.5 K [6]. Several other studies address the potential reduction in ambient temperature resulting from the use of reflective roofs [7,8]. For US cities with populations exceeding 100,000, it is projected that the peak electricity load will rise by 1.5–2% for each 1 °F increase in surrounding temperature [9].

A recent review article emphasizes the effectiveness of cool roofs in lowering both roof surface and surrounding temperatures, leading to energy savings through reduced cooling loads [10]. Also, in warm climates, under clear sky conditions, the surface temperature of crystalline PV panels, which typically have an albedo lower than 0.1, may surpass 70°C-80°C [11]. The performance of photovoltaic (PV) panels is significantly influenced by the temperature of their modules. Generally, the efficiency of a module made of crystalline silicon cells decreases by about 0.45% with every 1°C increase in temperature [12]. With the application of cool roofs, a cooler temperature underneath the PV module results in an increase in performance of the solar panel.

1.3 Heat transfer on the roof

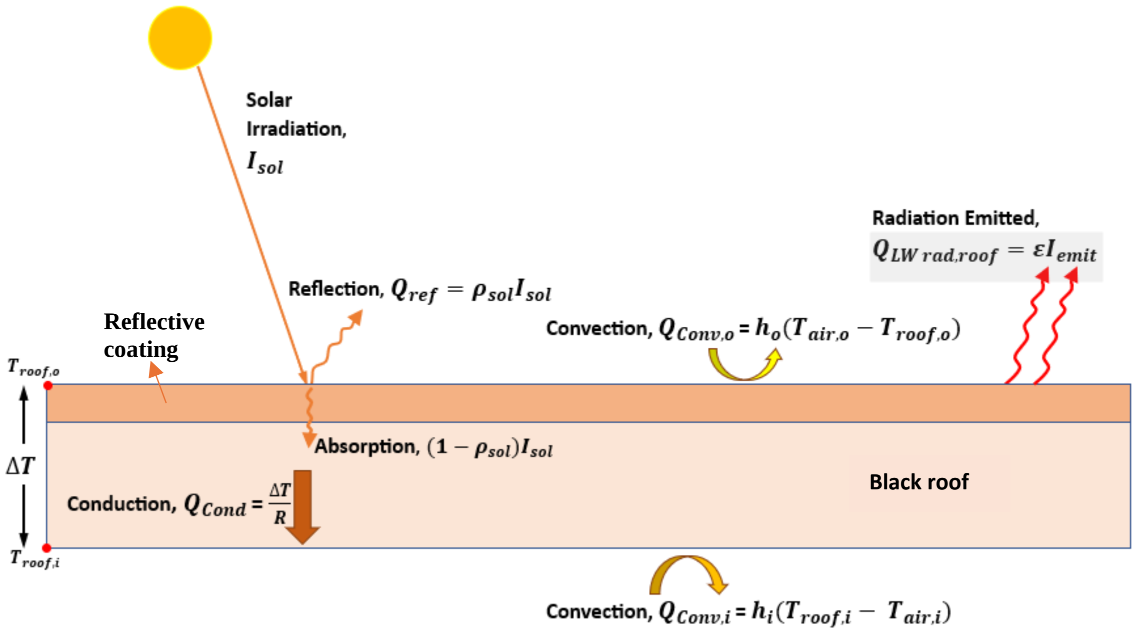

Figure 1-3: Heat Transfer on the Roof with Reflective Roof Coating (shown in dark color)

In Figure 1-3, the incoming radiation on the roof consists of short-wave radiation ranging from 250 nm to 3500 nm representing solar irradiation and radiation reflected by earth surfaces and long waves with wavelengths exceeding 3500 nm representing thermal radiation emitted by clouds and other terrestrial bodies. As depicted in Figure 1-3, part of the radiation incident on the roof is absorbed and the rest is reflected back to the atmosphere. Reflective roof coatings play an important role in reflecting the greater proportion of this radiation. A portion of the absorbed solar radiation dissipates as heat in the form of convection and long-wave radiation into the environment. Another part of the absorbed heat is conducted into the building depending on the thermal resistance of the roof layers, and the outside and inside temperature of the roof surface.

1.4 Properties of coatings

The Cool Roof Rating Council (CRRC) [13], a nonprofit organization, offers a framework for assessing various cool roof materials and manages a directory for accessing their properties. Reflective roof coatings are characterized by three main properties:

a) Solar Reflectance (SR):

Solar Reflectance (SR) is a metric, representing the ratio of solar radiation reflected outward by the surface to the total solar radiation incident upon it. It ranges over a scale of 0 to 1, with 0 being perfectly absorptive and 1 being perfectly reflective.

b) Thermal Emittance (TE):

Thermal emittance, also known as emissivity, characterizes the extent to which a material releases the absorbed thermal energy in the form of long wavelength radiation. Materials with high TE values are effective in radiating heat back into the atmosphere, preventing excessive heat buildup. It also ranges on a scale of 0 to 1, with thermal emittance of 1 for a perfectly black body.

c) Solar Reflectance Index (SRI):

The Solar Reflectance Index (SRI) is a metric for assessing a surface capacity to reflect solar heat and release the absorbed heat thereby minimizing temperature rise. It combines solar reflectance and thermal emittance into a single value. Calculating the SRI involves comparing surface temperatures to those of standard white and black materials under specific conditions. Its value is calibrated in a way that assigns a value of 0 to a standard black surface (with a reflectance of 0.05 and emittance of 0.90), and a value of

100 to a standard white surface (with a reflectance of 0.80 and emittance of 0.90) [14]. This standardized scale allows comparative evaluations of surfaces, facilitating the assessment of their thermal performance based on their capacity to reflect solar heat.

1.5 Climate zones

Climate has a considerable impact on the energy consumption of buildings. To ensure that builders adhere to specific regulations effectively, energy codes and standards rely on well-defined climate zones. The American Society of Heating, Refrigerating and Air-Conditioning Engineers (ASHRAE) established a comprehensive framework comprising 17 defined climate zones as shown in Table 1-1. These zones serve as a means to encompass the wide range of climates found worldwide.

Table 1-1: ASHRAE Climate Zones [15]

Climate Zone	Temperature	Moisture	Classification Description
1A	Very Hot	Humid	Tropical Wet and Dry
1B	Very Hot	Dry	Arid Middle Latitude
2A	Hot	Humid	Humid Subtropical (Warm Summer)
2B	Hot	Dry	Arid Subtropical
3A	Warm	Humid	Humid Subtropical
3B	Warm	Dry	Semiarid Middle Latitude/Arid Subtropical/Highlands
3C	Warm	Marine	Dry Summer Subtropical (Mediterranean)
4A	Mixed	Humid	Humid Subtropical/Humid Continental (Warm Summer)
4B	Mixed	Dry	Semiarid Middle Latitude/Arid Subtropical/Highlands
4C	Mixed	Marine	Marine (Cool Summer)
5A	Cool	Humid	Humid Continental (Warm Summer)
5B	Cool	Dry	Semiarid Middle Latitude/Highlands
5C	Cool	Marine	Marine (Cool)
6A	Cold	Humid	Humid Continental (Warm Summer/Cool Summer)
6B	Cold	Dry	Semiarid Middle Latitude/Highlands
7	Very Cold	-	Humid Continental (Cool Summer)
8	Subarctic	-	Subarctic

Figure 1-4 shows the map of United States divided into various climate zones by the International Energy Conservation Code (IECC) [16].

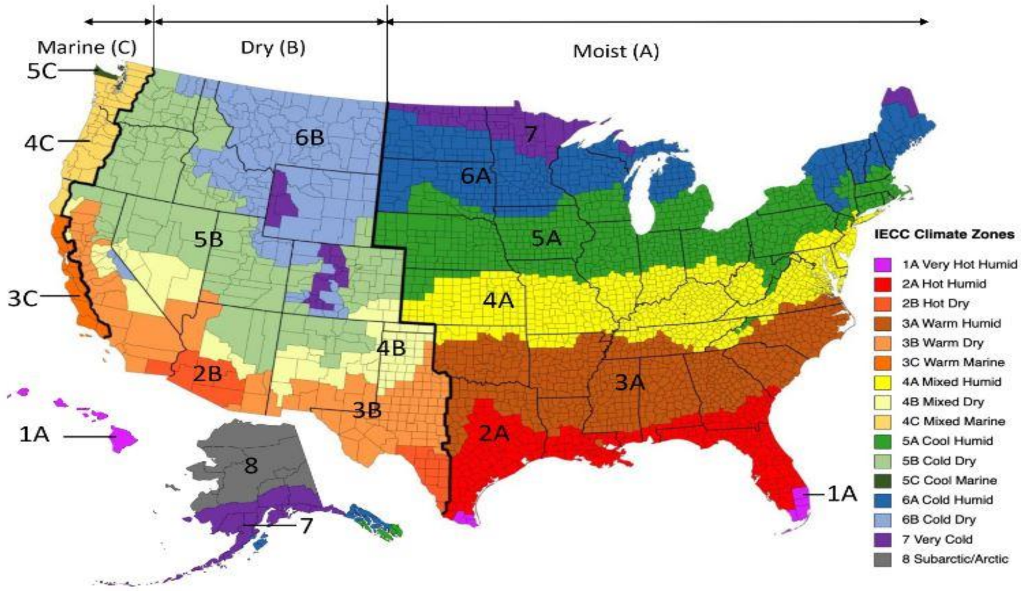

Figure 1-4: IECC Climate Zone Map [16]

1.6 About EnergyPlus

EnergyPlus™ is a whole building energy simulation program that engineers, architects, and researchers use to model both energy consumption—for heating, cooling, ventilation, lighting and plug and process loads—and water use in buildings [17]. Building upon the popular features of BLAST and DOE-2, EnergyPlus incorporates various innovative simulation capabilities. Initially funded by the United States Department of Energy (DoE) in 1996, its development has been a collaborative effort involving the National Renewable Energy Laboratory (NREL) and several National Laboratories like Lawrence Berkeley National Laboratory (LBNL) and Oak Ridge National Laboratory (ORNL). The software was first released in 2001, with subsequent continuous updates.

Some of the notable features and capabilities of EnergyPlus include [17]:

- Integrated, simultaneous solution of thermal zone conditions and HVAC system response that does not assume that the HVAC system can meet zone loads and can simulate un-conditioned and under-conditioned spaces.
- Heat balance-based solution of radiant and convective effects that produce surface temperatures, thermal comfort, and condensation calculations.
- Sub-hourly, user-definable time steps for interaction between thermal zones and the environment, with automatically varied time steps for interactions between thermal zones and HVAC systems. These allow EnergyPlus to model systems with fast dynamics while also trading off simulation speed for precision.
- Combined heat and mass transfer model that accounts for air movement between zones.
- Advanced fenestration models including controllable window blinds, electrochromic glazing, and layer-by-layer heat balances that calculate solar energy absorbed by window panes.
- Illuminance and glare calculations for reporting visual comfort and driving lighting controls.
- Component-based HVAC that supports both standard and novel system configurations.
- A large number of built-in HVAC and lighting control strategies and an extensible runtime scripting system for user-defined control.

- Functional Mockup Interface import and export for co-simulation with other engines.
- Standard summary and detailed output reports as well as user definable reports with selectable time-resolution from annual to sub-hourly, all with energy source multipliers.

EnergyPlus is tested according to ASHRAE Standard 140 methodology [18]. In 2003, EnergyPlus has been recognized with an R&D 100 award [19]. As a robust, freely accessible, and open-source software, it has emerged as the prevailing industry standard for both academic researchers and building professionals.

Similar to DOE-2, EnergyPlus features a simulation engine with a built-in modeler, which operates via a console-based interface, handling input and output through text files. With the help of a number of tools, users may manage input and output files, generate input files using a streamlined interface akin to a spreadsheet, run batch simulations, and graphically compare various outcomes. However, EnergyPlus's main graphical user interface is not user-friendly; it lacks graphic features and automation in the data tables used to manage building inputs and outputs. To make it user-friendly, various external graphic user interfaces and modelers have been developed. Examples include Autodesk Revit with Insight [20], Rhino [21], and Grasshopper [22] with Honeybee [23], SketchUp with OpenStudio [24], direct modeling and editing of building energy models (BEM) in OpenStudio [25], and DesignBuilder [26], among others.

Assumptions – EnergyPlus

Some of the assumptions [27] that EnergyPlus is based upon are:

a) **Gray Surfaces:** EnergyPlus assumes that all surfaces are gray, meaning they have constant emissivity and absorptivity values across all wavelengths. This simplification allows for simpler calculations compared to modeling surfaces with wavelength-dependent properties.

   - Each surface emits or reflects diffusely and is gray and opaque ($\alpha = \varepsilon$, $\tau = 0$, $\rho = 1 - \varepsilon$)
   - Energy flux leaving a surface is evenly distributed across the surface.

b) **Uniform Surface temperatures:** The inside and outside face of each surface has a single uniform surface temperature calculated from the surface heat balance.

c) **Constant Material Properties:** EnergyPlus assumes that material properties, such as thermal conductivity and heat capacity, remain constant throughout the simulation period. It does not account for variations in material properties with temperature or other factors.

d) **Homogeneous Spaces:** EnergyPlus assumes that each thermal zone within a building is homogeneous, meaning that the air temperature, humidity, and other conditions are uniform throughout the zone. It does not account for temperature stratification or variations within a zone.

e) **Solar Irradiance:**

   - The software assumes uniform solar irradiance over the external surfaces.

- The building surfaces are assumed to be diffusely reflecting if they are opaque (roofs, walls, for example) and specularly reflecting if they are windows or glass doors.

f) **Weather Data:** EnergyPlus relies on weather data to simulate the outdoor conditions affecting the building. It provides access to a wide range of weather data sources for 3,034 locations in 98 countries [28].

g) **Uniform Internal Heat Gains:** The software assumes that internal heat gains from occupants, lighting, and equipment are evenly distributed throughout a thermal zone. It does not consider localized heat sources or variations in heat generation within a zone.

h) **Occupants Heat Gain**: People count is usually hard to measure in reality, which results in simplification of occupancy schedule assumptions in energy modeling.

CHAPTER 2

Effect of Reflective Roof Coatings in Buildings

2.1 Model description

The study focuses on two of the Department of Energy's (DOE) prototype commercial buildings namely a standalone retail building of area 2,294 m^2 (24,692 ft^2) and a strip-mall of area 2,090 m^2 (22,500 ft^2) to simulate the impact of coatings [29]. The 3-D geometry of the standalone retail and the strip-mall building is shown in Figures 2-1 (a) and (b), respectively. The analysis in this study focuses on four distinct climatic conditions, specifically Phoenix, AZ (climate zone 2B), Houston, TX (climate zone 2A), Los Angeles, CA (climate zone 3B coast), and Miami, FL (climate zone 1A). TMY-3 weather files from EnergyPlus were employed to define the weather conditions for the annual simulations conducted across all four cities in this study [28].

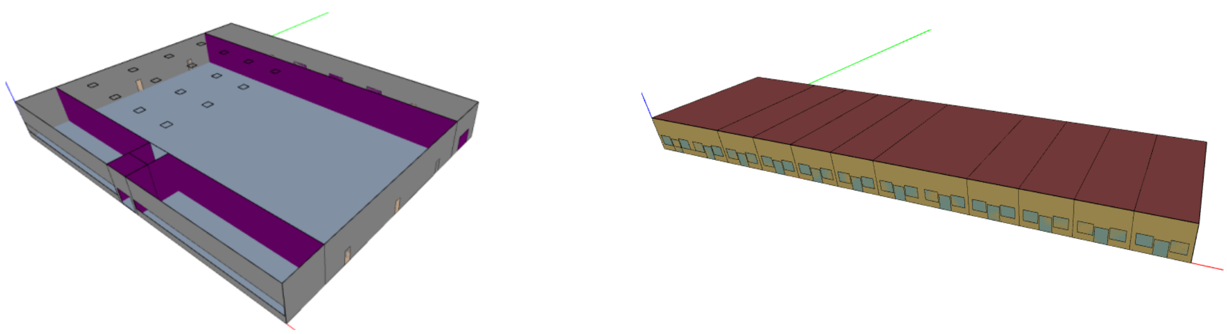

(a) (b)

Figure 2-1: DOE Prototype Buildings (a) Standalone retail (b) Strip-mall

In order to validate the findings, another tool, namely the ORNL Cool Roof Calculator [30] developed by DOE's Oak Ridge National Laboratory was utilized. The calculator compares cooling and heating load savings for flat roof with non-black surfaces. Based on that specific modifications were made to both the buildings as follows:

1. The R-value of the roof is adjusted to 1.76 m^2 K W^{-1} (10 h·ft²·°F Btu^{-1}) aligning with the average R-value provided by the ORNL Cool Roof Calculator. Additionally, the solar reflectance and thermal emittance of the roof are modified to 0.05 and 0.9 respectively, effectively simulating a black roof.

2. The Coefficient of Performance (COPs) of all the air conditioners (ACs) were modified to 2. This is the average value of the COP for an AC as given by the ORNL Cool Roof Calculator.

3. The heating is provided by natural gas furnaces, with their efficiencies modified to 0.7 - consistent with the average efficiency of a gas furnace as per the ORNL Cool Roof Calculator.

The assessment of the performance of roof coatings involves applying an additional layer over the baseline black roof, characterized by a solar reflectance of 0.05 and a thermal emittance of 0.9. This is pictorially shown in Figure 1-3. These properties of the black roof are chosen as a standard by Oak Ridge Cool Roof Laboratory to evaluate performance of a coating [30]. Table 2-1 provides an overview of the properties of commonly used commercial silicone, acrylic, and aluminum coatings available in the market. In Table 2-1, C-1 is a 100% silicone, moisture-cure coating. C-2, C-3, and C-4 are 100% acrylic white extreme elastomeric roof coatings, C-5 is fibered aluminum roof coating and C-6 is an acrylic polyurethane white waterproof roof coating.

Table 2-1: Material Properties of Coatings

Properties	C-1	C-2	C-3	C-4	C-5	C-6
Solar reflectance	0.87	0.86	0.84	0.86	0.53	0.83
Thermal emittance	0.9	0.9	0.91	0.88	0.5	0.91
Number of coats#	1	2	2	2	2	2
Thickness of single coat (mm)	0.407	0.407	0.407	0.407	0.407	0.407
Thermal conductivity (W m^{-1} K^{-1})	0.63	0.19	0.19	0.19	237	0.67
Density (kg/m^3)	1210	1426	1408	1408	935	1307
Specific heat (J kg^{-1} K^{-1})	1147	1248	1248	1248	900	1253

suggested by the manufacturer

2.2 Net HVAC energy saving comparison in four US locations

The comparative analysis presented in Figures 2-2 (a) to (d) offers insights into the net savings in HVAC energy consumption resulting from the application of different types of reflective roof coatings in the four geographic locations for both standalone retail and strip-mall buildings. Net savings are determined by subtracting the energy penalty incurred during heating from the energy savings achieved during cooling. The results are normalized by floor area, making it possible to apply them to other buildings with different areas, provided they have similar characteristics in terms of construction, HVAC type, and building loads. Notably, Miami exhibits the highest level of savings for both standalone retail and strip-mall buildings followed by Phoenix. It can also be observed that buildings in Houston and Los Angeles exhibit comparable levels of net HVAC load savings, making them comparable in this aspect.

The efficacy of a coating is significantly influenced by its solar reflectance and thermal emittance values. As can be noted from Figure 2-2 the performance of coating C-5 is worst as compared to others because of its lower solar reflectance and thermal emittance values. Given that the HVAC load per square foot varies depending on the size and type of a building, slight variations in the net savings per square foot for the standalone and strip-mall buildings across all locations for all the coatings, can also be observed.

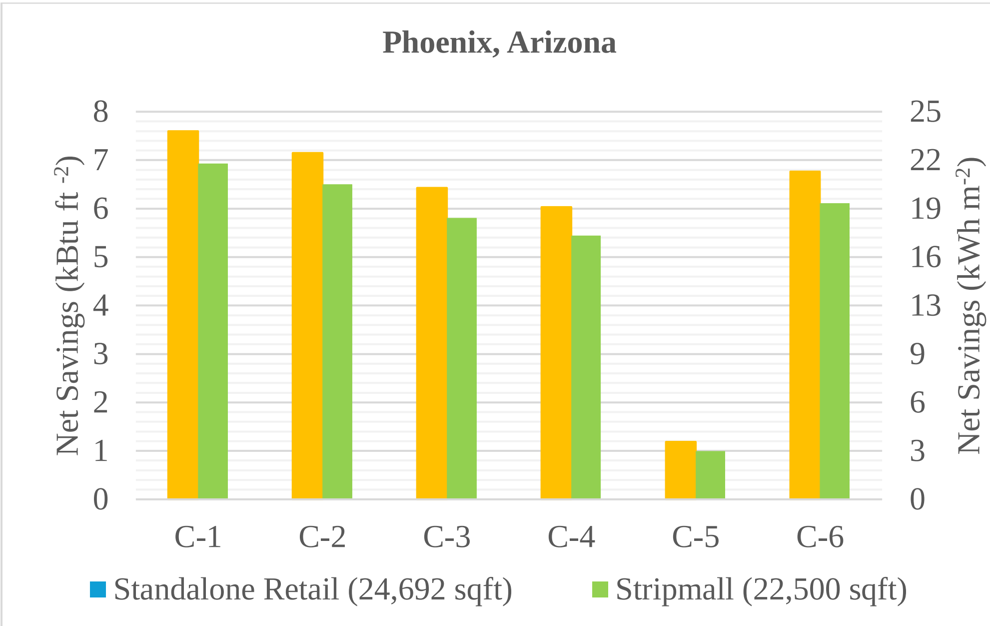

Figure 2-2(a)

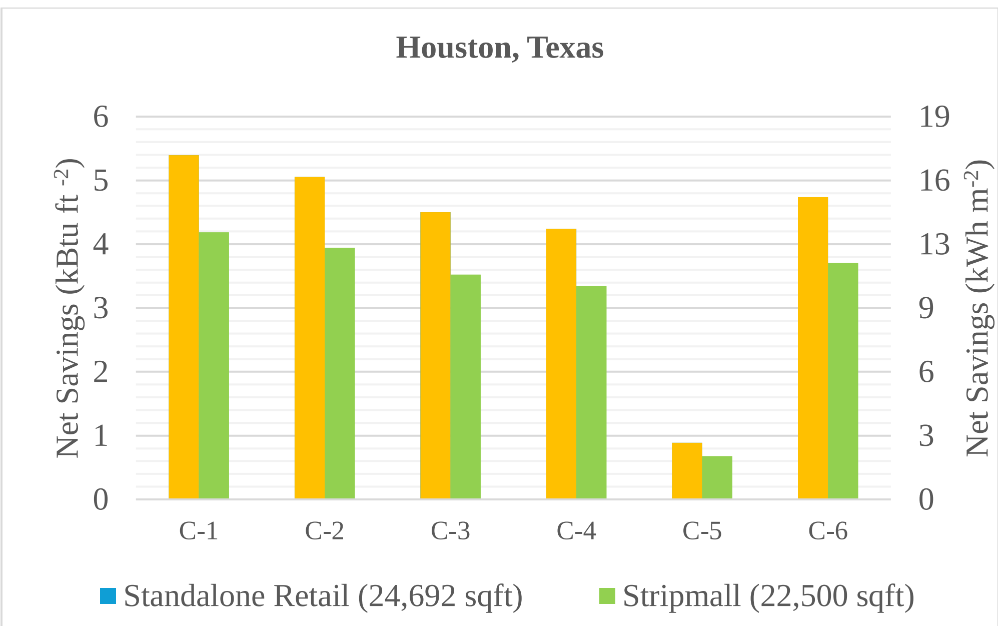

Figure 2-2(b)

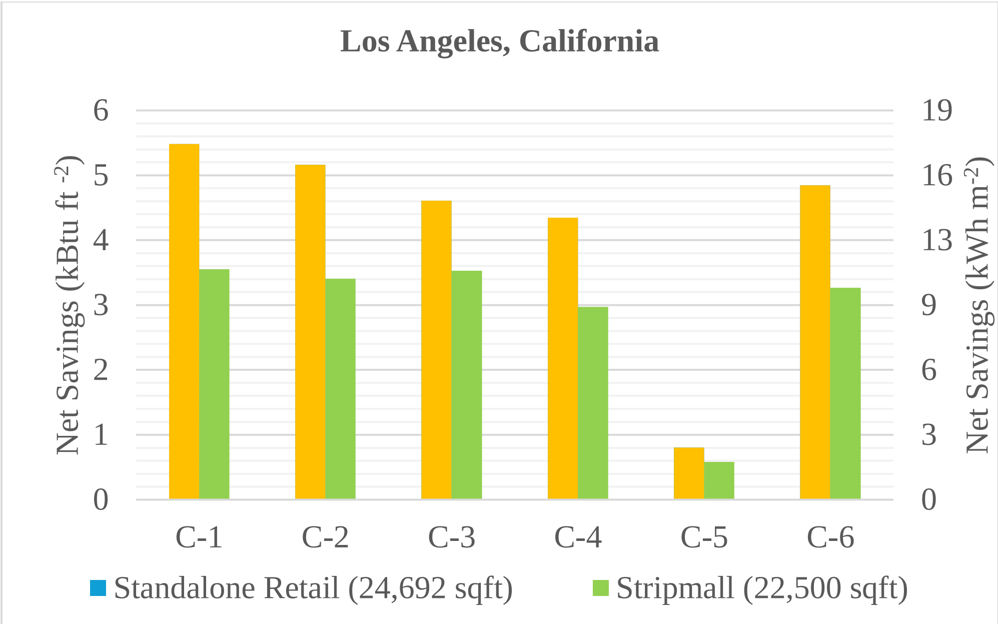

Figure 2-2(c)

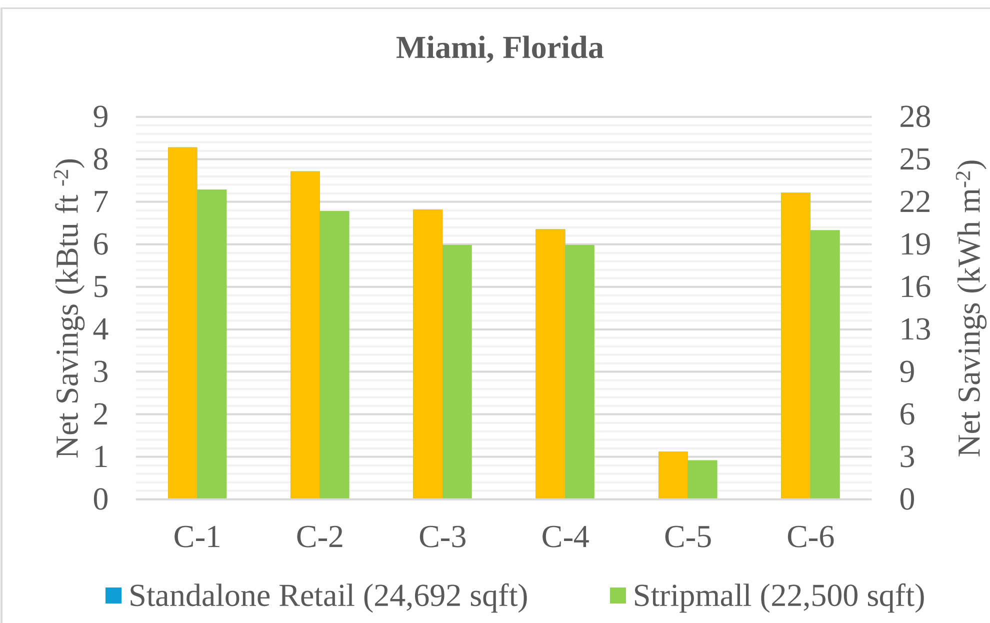

Figure 2-2(d)

Figure 2-2(a) to (d): Location-wise Net Savings in HVAC Energy for Different Coatings

2.3 Effect of solar reflectance and thermal emittance on roof temperatures

In order to examine the impact of solar reflectance and thermal emittance on roof surface temperatures, hourly temperatures on the 8th of August in Phoenix - a day characterized by the highest average temperature according to EnergyPlus TMY3 data, were analyzed. As illustrated in Figure 2-3, an uncoated black roof can reach up to temperatures of 93.3°C (200ºF) in the afternoon, nearly double the ambient air temperature at that time. With the application of a coating, an increase in the solar reflectance value of the coating results in lower roof temperatures during daylight hours. Remarkably, super cool roofs having a solar reflectance value close to 1 can achieve temperatures below ambient during all the times of the day. However, such higher values of solar reflectance are challenging to attain and maintain due to the accumulation of dust and dirt over a period of time. While the commercially available cool roof materials typically exhibit a maximum solar reflectance of 0.86 and an emissivity of 0.9, recent studies unveiled materials that can possess an exceptionally high albedo exceeding 0.95, along with high thermal emissivity exceeding 0.95 as well [31, 32, 33].

It is interesting to note that during nighttime, roof temperatures are generally less than the ambient temperature. This is the result of a phenomenon known as *nocturnal cooling*, also called night sky cooling. It is the cooling of a building by long wavelength radiation to the night sky. Building roofs emit heat continuously, releasing at a rate of up to 75 W/m^2 day and night [34]. While this heat loss is counteracted by solar radiation gains during the day, it has the potential to reduce roof temperatures by 6 to 20°C below ambient levels during the night [34].

Key factors affecting the rate of nocturnal cooling (*NC*) include:

i.	Emissivity of the surface	$\epsilon \uparrow \ NC \uparrow$
ii.	Sky conditions (Clear, Cloudy)	sky clearness $\uparrow \ NC \uparrow$
iii.	Humidity	$\omega \uparrow , NC \downarrow$
iv.	Wind speed	$v \uparrow$, $convection\ HT \uparrow$, NC ↑
v.	Thermal mass	$mC_p \uparrow$, $ability\ to\ retain\ heat \uparrow$, $NC \downarrow$
vi.	Geographical location	$Night\ time \uparrow$, $NC \uparrow$

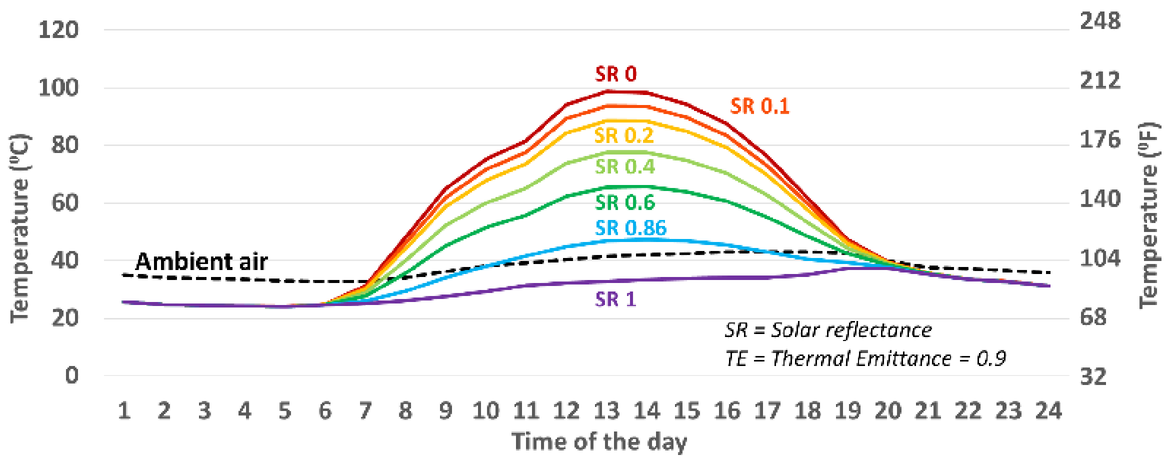

Figure 2-3**:** Effect of Solar Reflectance on Roof Surface Temperature at Constant Thermal Emittance on 8th Aug for Phoenix, AZ

Similarly, as illustrated in Figure 2-4, at a constant solar reflectance of 0.86, the thermal emittance of the coating is varied on the same day (8th Aug) in Phoenix. It can be observed that lower thermal emittance values approaching zero can result in roof temperatures over 60°C (140ºF) in the afternoon when the ambient temperature is around 43°C (110ºF). A higher thermal emittance of the coating can bring roof temperatures close to ambient during the daytimes. During night hours, it can be seen that higher temperature drop in roof temperature occurs at higher values of thermal emittance. This phenomenon can be attributed to the same nocturnal cooling discussed earlier.

It can also be noted that temperature at approximately zero thermal emittance is at least 40°C (104ºF) less than the temperature in the case when solar reflectance is zero as can be compared with Figure 2-3. This highlights the significant influence of solar reflectance over thermal emittance in governing roof temperatures.

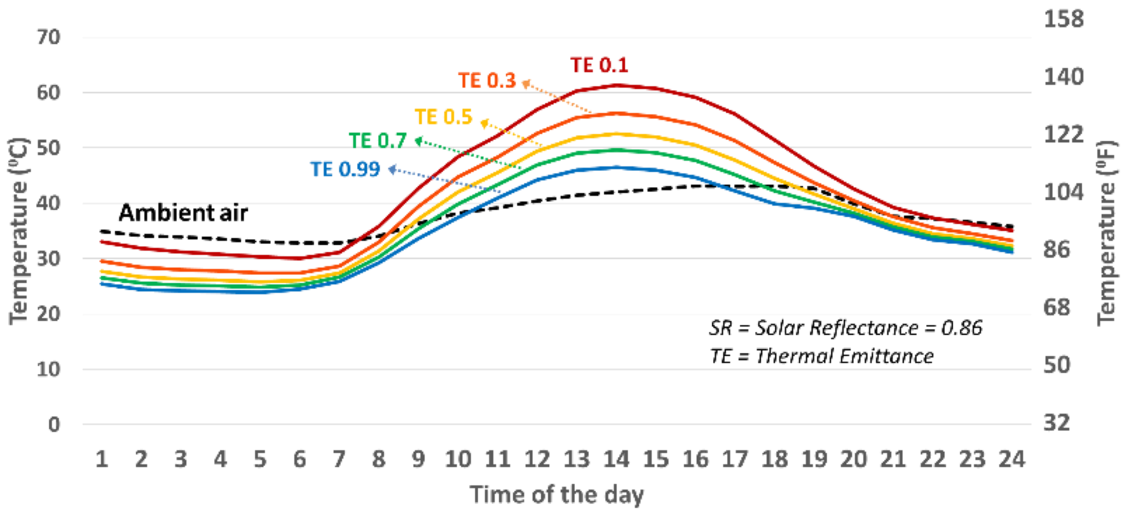

Figure 2-4**:** Effect of Thermal Emittance on Roof Surface Temperature at Constant Solar Reflectance on 8th Aug for Phoenix, AZ

Reduced temperature of the roof with the application of coatings having high solar reflectance and thermal emittance is the primary reason behind the reduced cooling needs in the buildings.

2.4 Effect of solar reflectance and thermal emittance on HVAC energy Consumption

To analyze the impact of the combination of solar reflectance and thermal emittance on roof coating performance, contour plots for annual savings in cooling energy and penalty in heating energy, as shown in Figure 2-5 and Figure 2-6, are generated for a standalone retail commercial building in Phoenix, Arizona. These plots offer insights into how specific values of solar reflectance and thermal emittance impact the building's cooling and heating requirements. Savings or penalty is with respect to the baseline black roof (indicated by a black dot in Figures 2-5, 2-6 and 2-7) with solar reflectance 0.05 and thermal emittance 0.9. As previously discussed in Section 2.1, these properties of the black roof are chosen as a standard by Oak Ridge Cool Roof Laboratory to evaluate performance of a coating [30]. It is evident that higher values of both solar reflectance and thermal emittance result in reduced cooling demands but increased heating demands. Yet, in regions like Phoenix, where the cooling demand significantly outweighs the heating demand, as indicated by the color bars in the contour plots, these coatings can lead to substantial savings in energy costs. The quantification of net HVAC energy savings with respect to black roof is reported in Figure 2-7.

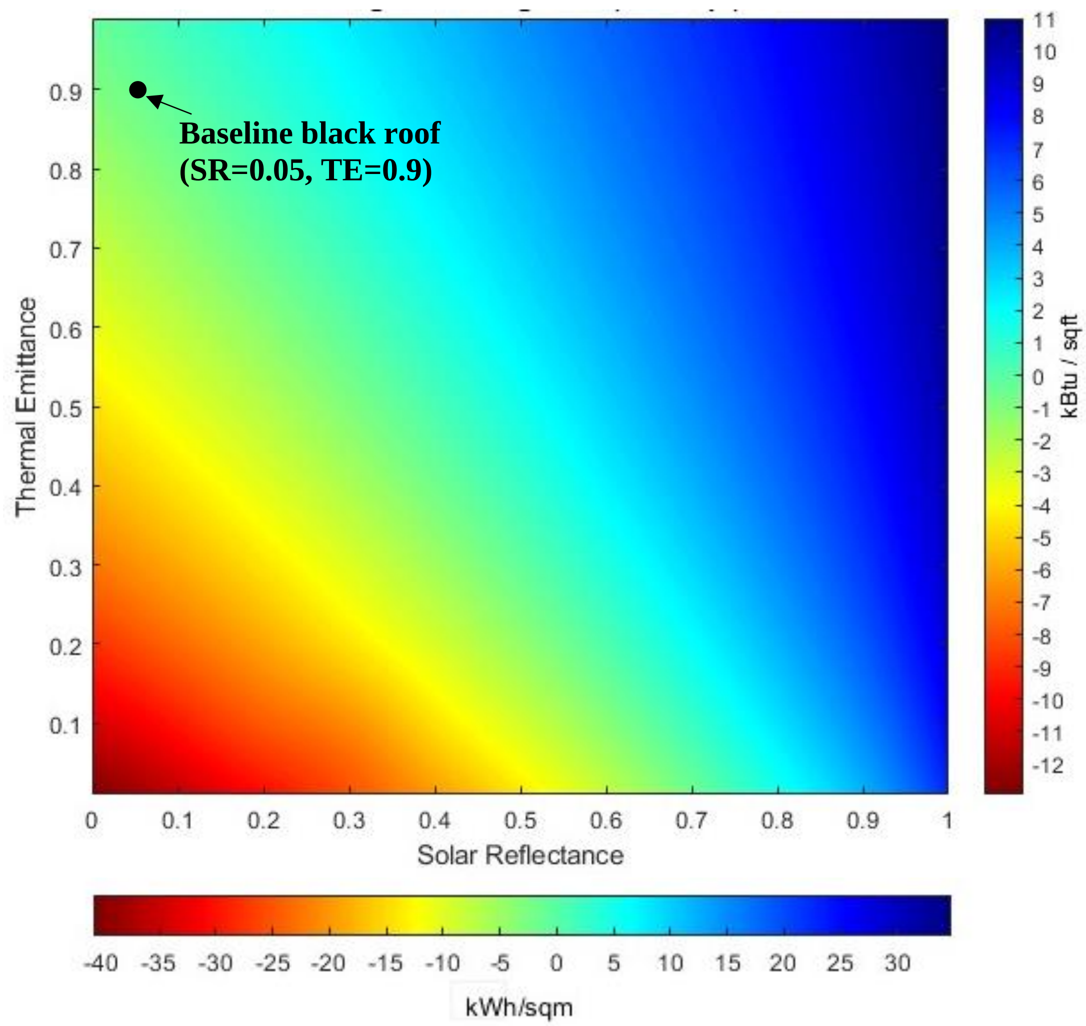

Figure 2-5**:** Effect of Solar Reflectance and Thermal Emittance on Annual Savings in Cooling Energy with Respect to Baseline Black Roof (SR=0.05, TE=0.9) for Phoenix, AZ

(* Negative values indicate cooling energy penalty with respect to baseline black roof)

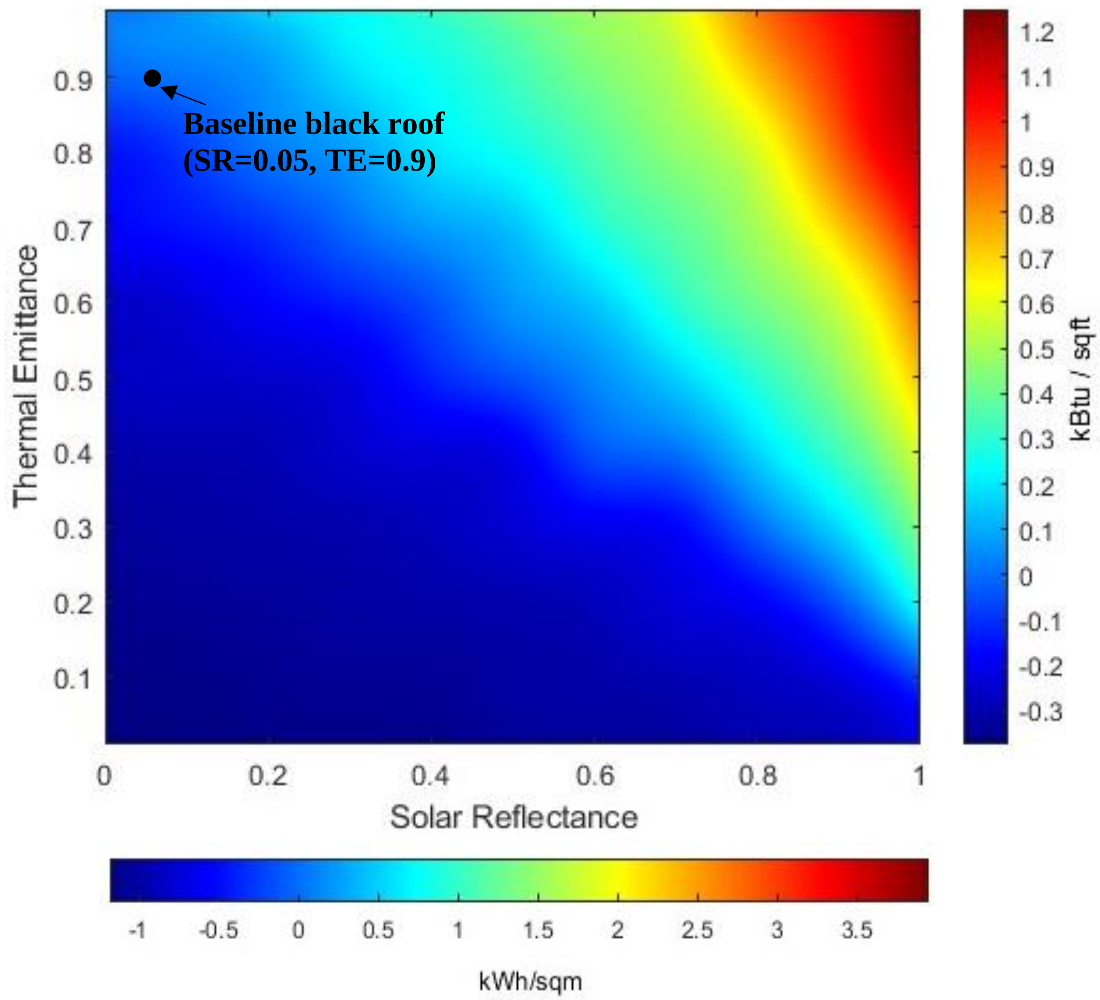

Figure 2-6**:** Effect of Solar Reflectance and Thermal Emittance on Annual Heating Energy Penalty with Respect to Baseline Black Roof (SR=0.05, TE=0.9) for Phoenix, AZ

(* Negative values indicate heating energy savings with respect to baseline black roof)

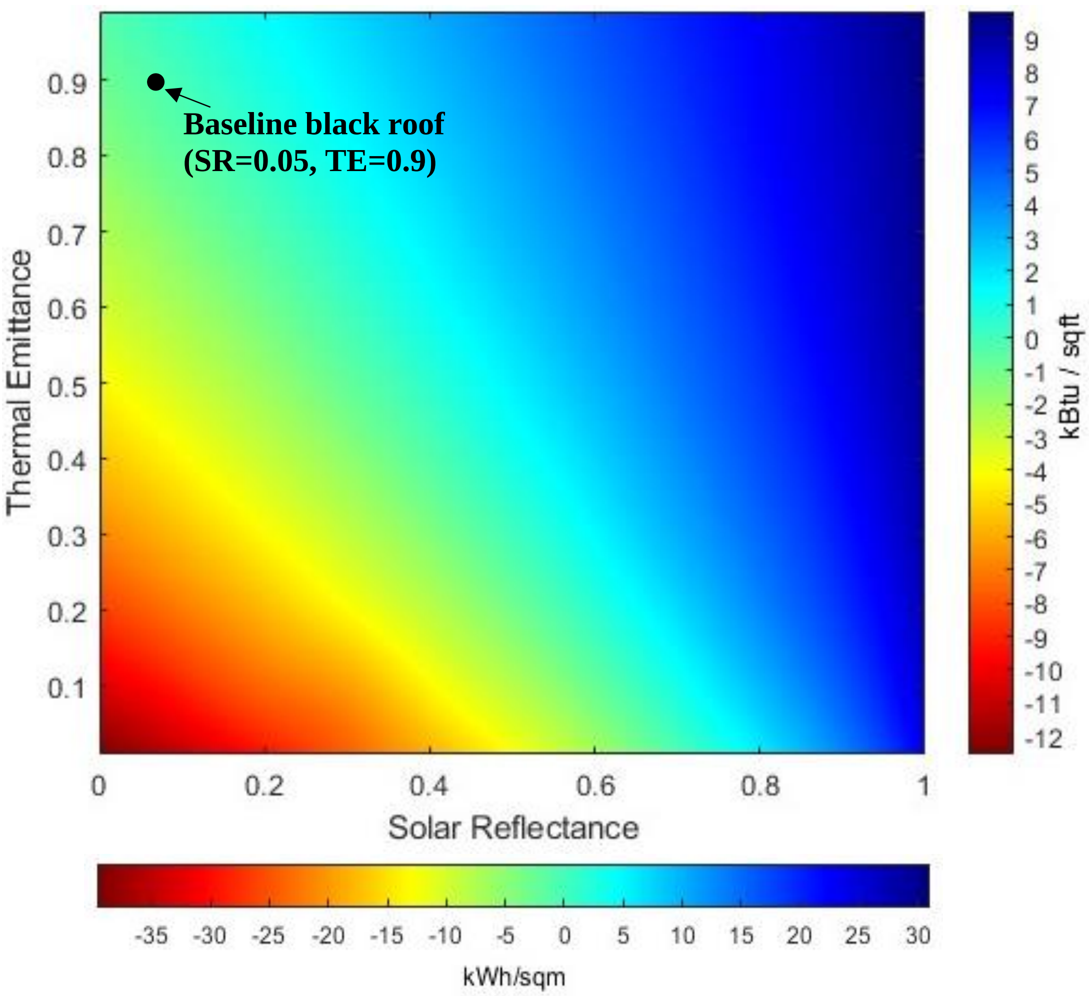

Figure 2-7**:** Effect of Solar Reflectance and Thermal Emittance on Net Annual Savings in HVAC Energy with Respect to Baseline Black Roof (SR=0.05, TE=0.9) for Phoenix, AZ

(* Negative values indicate net loss with respect to baseline black roof)

2.5 Reflective roof coatings vs roof thermal insulation

To explore the relationship between the insulation thermal resistance (R-value) of the roof and the resulting energy savings achieved by the application of reflective coatings, the following analysis has been done. This involves varying the insulation thermal resistance of the roof across a range from 1 m^2 K W^{-1} (5.6 ft^2 °F h Btu^{-1})to 5 m^2 K W^{-1} (28.4 ft^2 °F h Btu^{-1}), while applying three distinct coatings (one at a time) with solar reflectance values of 0.42, 0.73 and 0.84. This analysis was carried out on a strip-mall building situated in Phoenix, Arizona. ANSI/ASHRAE/IES Standard 90.1 [35] and IECC C402.1.3 [36] mandates a minimum roof R value of 25 ft^2 °F h Btu^{-1} (R-25) in buildings in climate zone 2 (Phoenix). This can have a significant impact on the energy savings that can be realized with the use of reflective coatings.

Figure 2-8 and Figure 2-9 respectively show the annual cooling energy consumption and corresponding percentage savings in cooling energy achieved by employing coatings of varying solar reflectance.

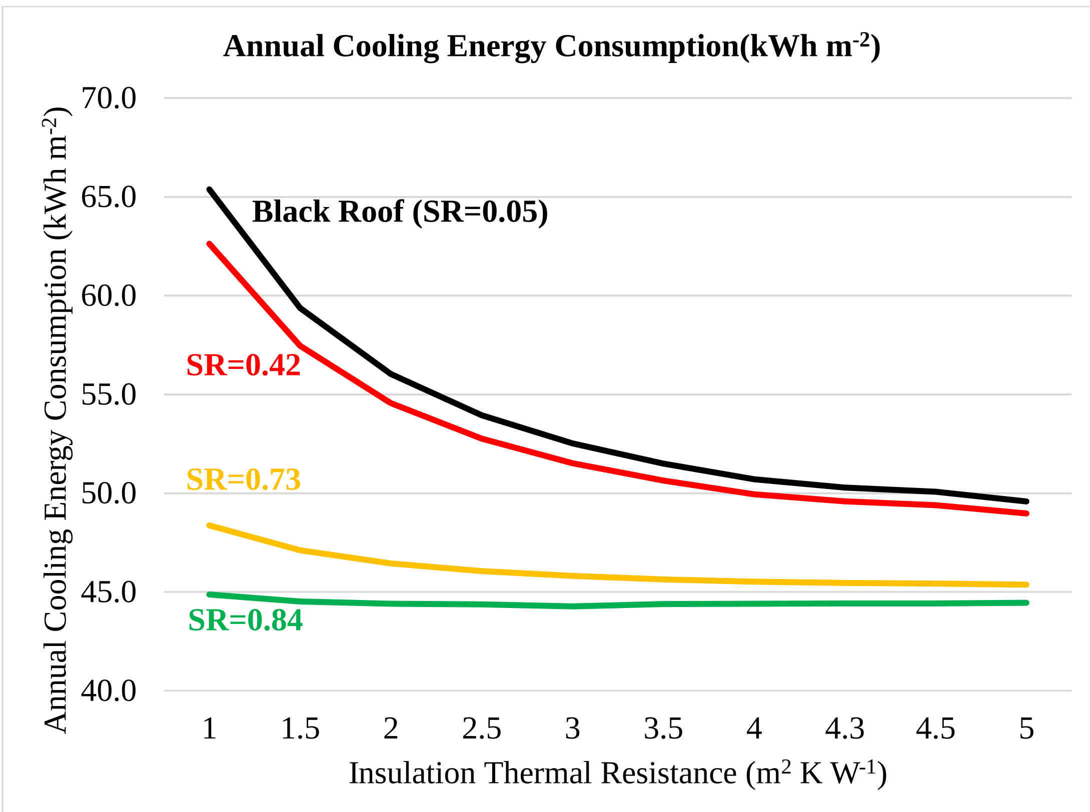

Figure 2-8: Effect of Insulation Thermal Resistance on Annual Cooling Energy Consumption for Coatings of Different Solar Reflectance (Phoenix, AZ)

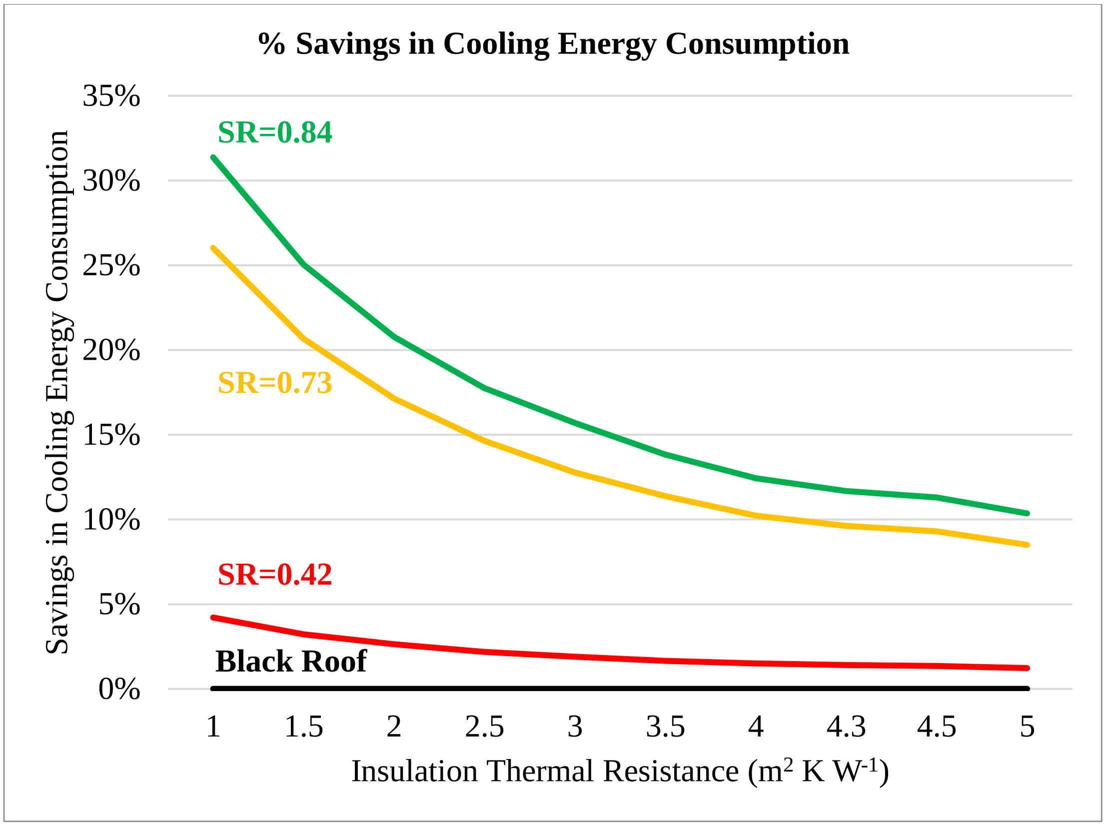

Figure 2-9: Effect of Insulation Thermal Resistance on % Savings in Annual Cooling Energy for Coatings of Different Solar Reflectance (Phoenix, AZ)

The following observations can be made after examining Figure 2-8 and Figure 2-9:

1. With an increase in solar reflectance value of the coating, the dependence of cooling energy on insulation thermal resistance of roof decreases. In an ideal situation with a perfect cool roof having a solar reflectance of 1, the graph would exhibit a horizontal trend i.e. cooling energy consumption would remain the same regardless of insulation.
2. For a black roof, there is a significant decrease in cooling energy consumption with an increase in insulation thermal resistance, and this reduction occurs at the highest rate when compared to other coatings. However, as depicted in Figure 2-

8, with higher solar reflectance values of the coating, the rate of decrease in cooling energy diminishes, as indicated by the lesser slope of the line graph.

3. All plotted line graphs for the reflective coatings converge with respect to the black roof. This convergence suggests that poorly insulated buildings can realize substantial energy savings through the application of coatings. For instance, a coating with a solar reflectance of 0.84 can result in approximately 30% reduction in cooling energy when the insulation thermal resistance of the roof is 1 m^2K/W, compared to only 10% reduction in cooling energy when the insulation resistance is 5 m^2K/W.
4. There exists a threshold value of insulation thermal resistance beyond which further increases have minimal impact on cooling energy reduction. Consequently, the savings derived from reflective roof coatings remain relatively constant beyond this point.

Similarly, Figure 2-10 illustrates the annual heating energy variations across different coatings applied to a strip mall building in Phoenix, Arizona.

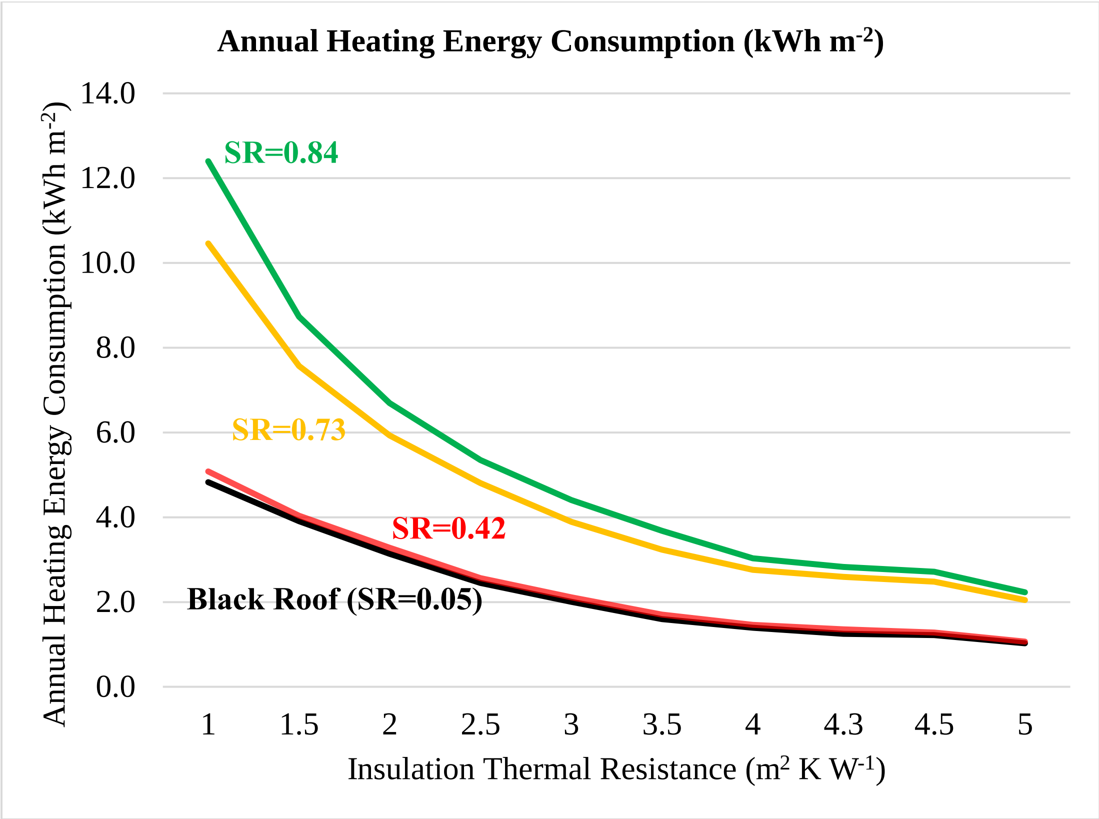

Figure 2-10: Effect of Insulation Thermal Resistance on Annual Heating Energy Consumption for Coatings of Different Solar Reflectance (Phoenix, AZ)

The pattern observed in annual cooling energy consumption plot in Figure 2-8 and the trends shown in Figure 2-10 about the effect of insulation thermal resistance on building heating energy consumption are similar. Higher solar reflectance coatings have a significant negative impact on heating energy consumption at lower insulation values. Plots converge towards the black roof as insulation levels rise, suggesting a decline in the heating penalty. However, it's worth noting that the magnitude of the heating penalty is relatively small compared to the savings achieved in cooling energy. For instance, considering a coating with a solar reflectance of 0.84 and insulation thermal resistance 1 m^2K/W, the heating penalty as compared to the black roof is approximately 7 kWh m^{-2}, while the savings due to reduction in cooling energy compared to the black roof are around 20 kWh m^{-2}. This results in overall savings of around 13 kWh m^{-2} under those conditions.

CHAPTER 3

Roof Coatings and Solar Panels: Impact on Building HVAC Demands

This chapter aims to evaluate the impact of roof reflective coatings on HVAC energy consumption in buildings installed with solar panels on the roof. EnergyPlus has the ability to model a simple photovoltaic (PV) system over the building that acts as a shading surface on the roof. By utilizing the capabilities of the simple photovoltaic module in EnergyPlus model, this study aims to understand the relationship between various solar reflectance values of roof reflective coatings and area fractions of PV system. To better understand this phenomenon, let us revisit the fundamental purpose of reflective coatings. Firstly, the coatings possess higher solar reflectance, enabling them to reflect short wavelength solar radiation effectively. Secondly, they have high thermal emittance values, which enables them to release absorbed heat in the form of long wavelength radiation at a faster rate. However, the presence of solar panels on the roof acts as a barrier to the exchange of this long-wavelength heat with the sky, thereby influencing the cooling load differently based on solar reflectance value of coating.

The following conditions are assumed in the calculations:

1. **Location:** Phoenix, Arizona
2. **Building:** Strip-mall (22,500 ft^2)
3. **R-value of roof:** 25 h ft^2 °F Btu^{-1}
4. **Black roof:** SR=0.05 and TE=0.9
5. **Thermal emittance of coating:** 0.9

Figure 3-1 and Figure 3-2 illustrate the impact of the area fraction of a PV panel on the surface temperatures of both the black roof and the coated roof (SR=0.84) respectively. The graphs are plotted for 8th Aug, a day characterized by highest average day temperatures. It can be observed that a black roof can reach temperatures more than 80°C during the day at a PV area fractions of 0.2. However, as the area fraction of the panel increases, the roof temperature decreases. Notably, the temperature variations with the coated roof are significantly narrower with respect to ambient, as depicted in Figure 3-2. At an area fraction of 1, both roofs exhibit similar temperature behaviors.

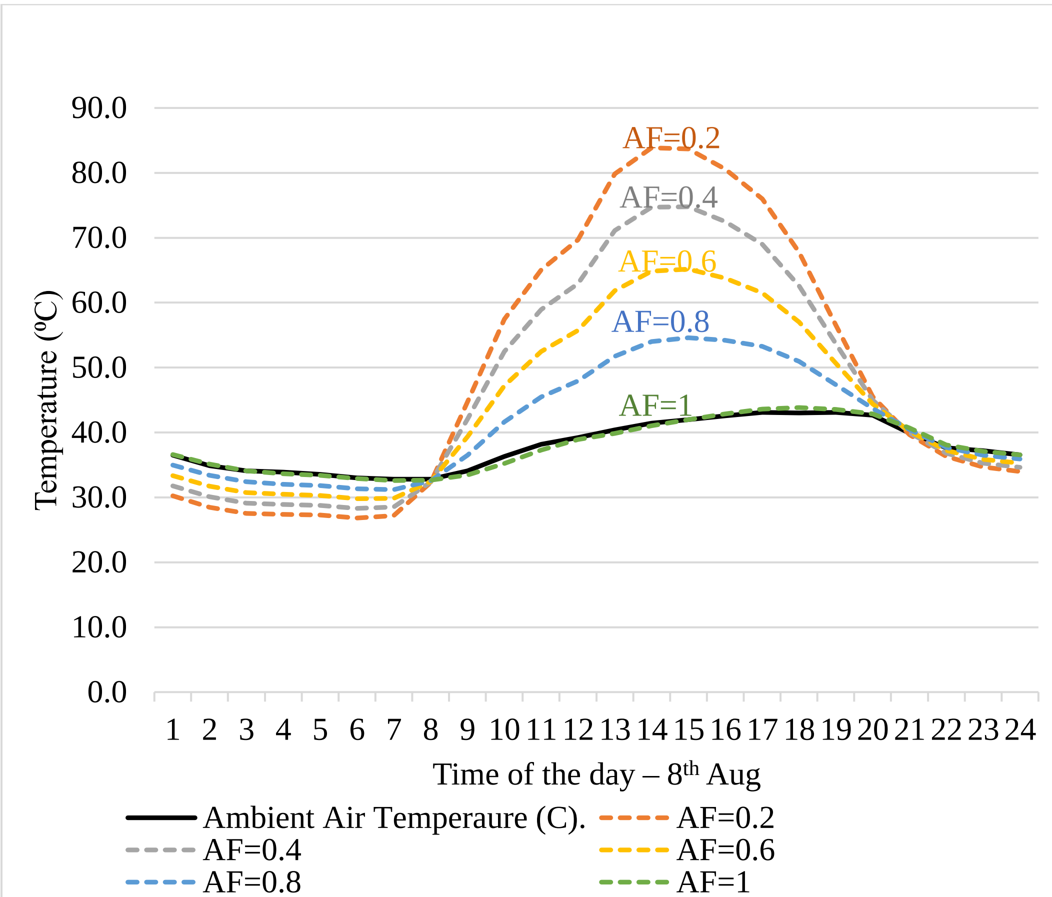

Figure 3-1: Effect of Area Fraction of PV on Surface Temperatures of the Black Roof on 8th Aug, in a Strip-mall Building in Phoenix, AZ

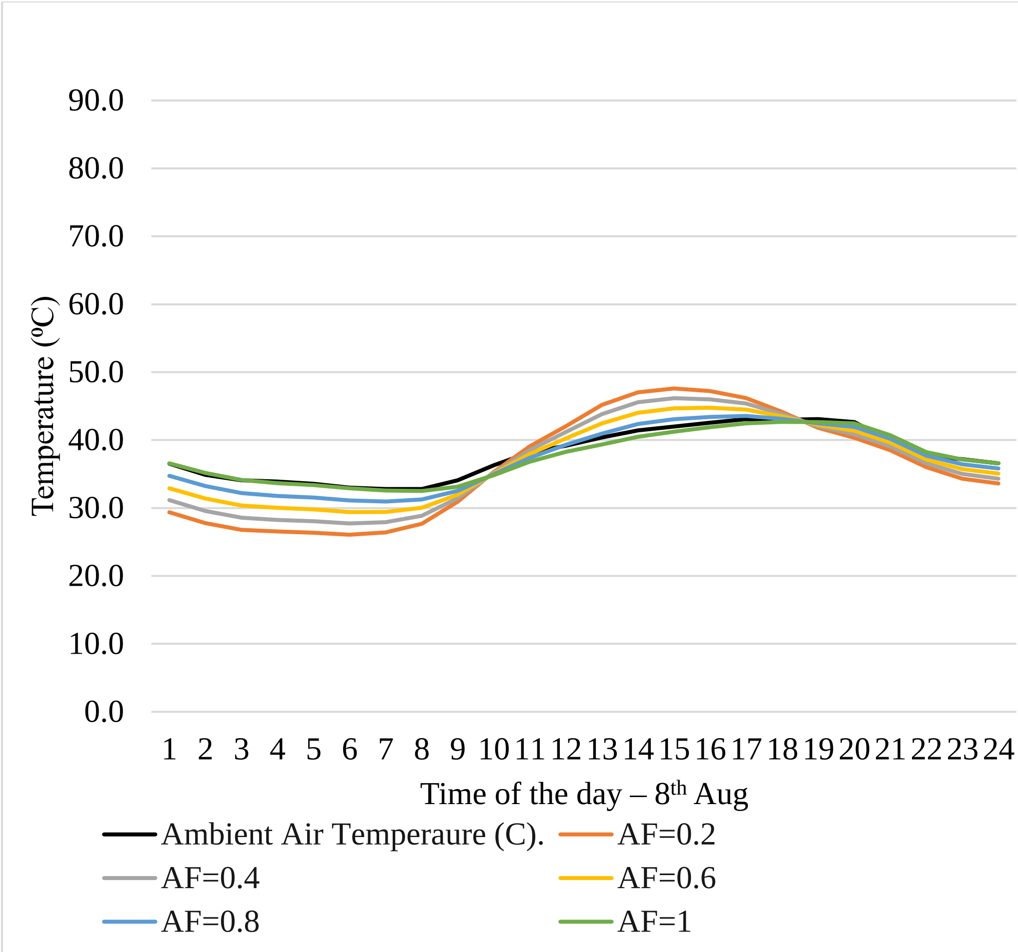

Figure 3-2: Effect of Area Fraction of PV on Surface Temperatures of the Coated Roof (SR=0.84) on 8th Aug, in a Strip-mall Building in Phoenix, AZ

Figure 3-3 provides insights into how annual cooling energy consumption varies at various area fractions of PV panel and solar reflectance of the coating.

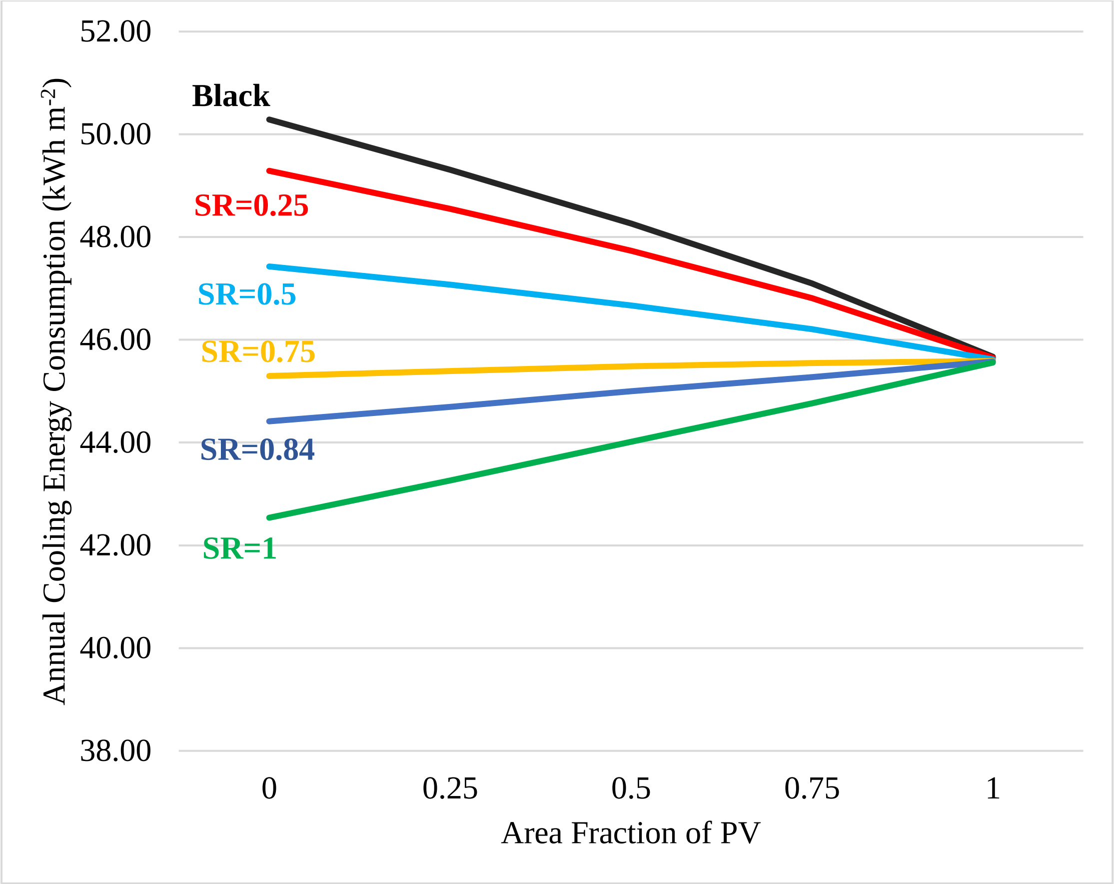

Figure 3-3: Effect of Area Fraction of PV and Solar Reflectance of Coating on Annual Cooling Energy Consumption of the Building

The following are the observations that can be made from Figure 3-3.

1. Notably, the cooling energy consumption of a building remains constant for an area fraction of 1, irrespective of the type of roof coating. This is attributed to the complete coverage of the roof by PV panels, preventing short-wavelength solar radiation from reaching the roof's surface. As a result, regardless of the type of coating on the roof, the cooling energy consumption in the building remains unaffected.
2. An important point to observe here is that there exists a threshold solar reflectance, somewhere around 0.75 above which the impact of area fraction is

opposite to the coating that has solar reflectance below this threshold. For the coating with solar reflectance greater than 0.75, the hinderance to their ability to release heat into the sky (due to PV) plays a dominant role than their ability to reflect solar radiation from the portion that has no PV. Above this solar reflectance, increasing the area fraction of PV traps the long wavelength radiations at a rate higher than the rate at which short wavelength radiations are absorbed into the roof (from non-PV portion), resulting in an increase in cooling energy consumption. Conversely, for coatings with solar reflectance less than 0.75 including the black roof, the rate at which heat is being absorbed into the roof from the non-PV portion has dominance over the long wavelength heat that is being trapped by PV panels. Hence, increasing the area fraction of PV leads to decrease in the cooling energy consumption. However, generalizing this threshold for all buildings is not feasible, as its value depends on various factors such as location, building construction, HVAC system type, among others.

3. Black roofs consistently exhibit inferior performance compared to reflective roofs, except at an area fraction of 1. However, it can also be noted that the amount of savings in cooling energy at higher area fractions of PV is less as compared to lower area fractions. For instance, a coating with a solar reflectance of 0.84 can achieve approximately a 9% reduction in cooling energy at an area fraction of 0.25, whereas the reduction is only 4% at an area fraction of 0.75.

Similarly, Figure 3-4 shows the influence of varying area fractions and solar reflectance of a reflective roof coating on the annual heating energy consumption of a strip-mall building in Phoenix, Arizona.

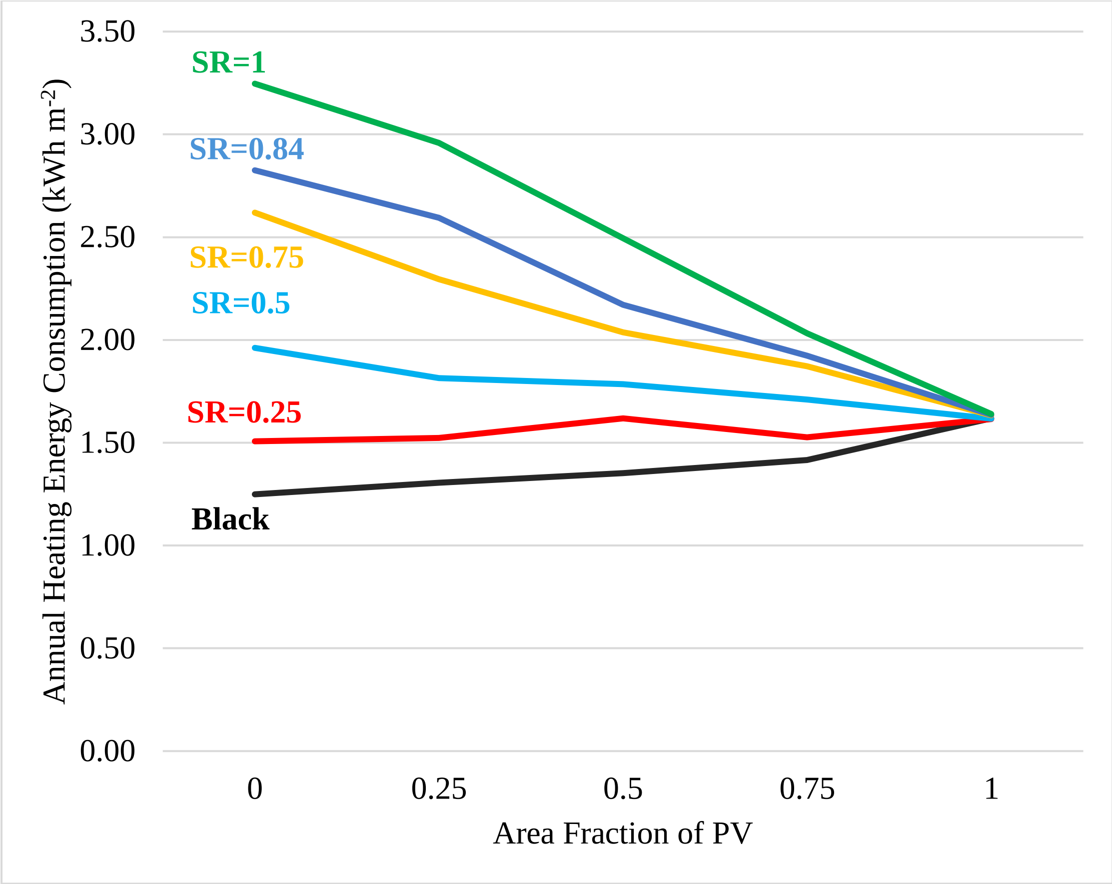

Figure 3-4: Effect of Area Fraction of PV and Solar Reflectance of Coating on Annual Heating Energy Consumption of the Building

It can be observed that the annual heating energy consumption plot is exactly the reverse of the cooling energy consumption plot. High reflectance coatings are associated with more heating penalties compared to black roof. The heating penalty decreases as the area fraction of PV is increased. The magnitude of heating penalty is small as compared to savings in cooling energy as indicated by Figure 3-3, resulting in overall savings. Similar to the cooling energy consumption, coatings don’t have any impact on heating energy consumption at an area fraction of 1.

Figure 3-5 illustrates the variation in annual cooling energy consumption for a building with and without PV panels, assuming a 75% area fraction of PV. The graph represents a strip-mall building located in Phoenix, Arizona.

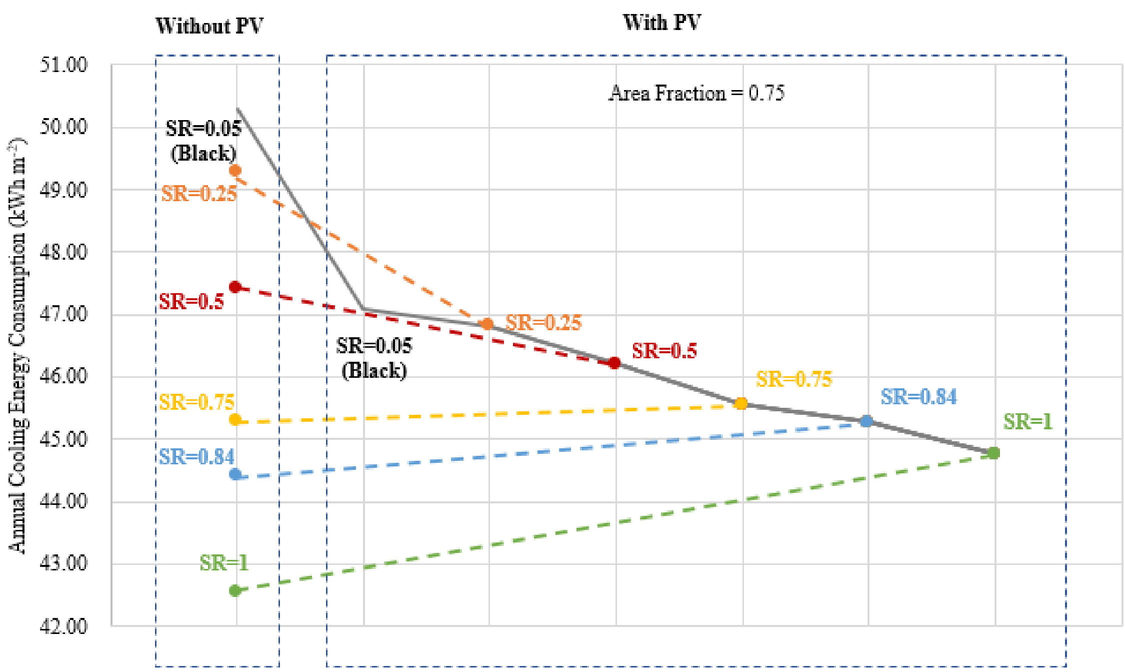

Figure 3-5: Comparison of Annual Cooling Energy Consumption of the Building With and Without Solar Panels for Different Coatings

Key observations from the plot include the following:

1. When a roof possesses a solar reflectance value approximately less than 0.75, the introduction of PV panels over the roof leads to a reduction in cooling energy consumption. As discussed previously, the heat that is being absorbed into the low reflectance roof without PV is much higher than the heat being trapped due to PV in the form of long wavelength radiation i.e. with the addition of PV panels, there is a large reduction in short wavelength radiations from the sun absorbed by the roof, resulting in reduction in cooling energy consumption.

2. Conversely, for roofs that have a solar reflectance approximately greater than 0.75, adding PV panels results in an increase in cooling energy consumption.
3. Another important point to note is that when the building has PV installed on it, adding a better reflective coating is always beneficial, leading to a reduction in cooling energy consumption. For instance, in Figure 3-5, for a black roof with PV panels (AF=0.75), the cooling energy consumption is 47 kWh m^{-2}. Increasing the solar reflectance to 0.84 reduces the cooling energy consumption to 45 kWh m^{-2}, representing approximately a 4% savings in cooling energy.

CHAPTER 4

Effect of Roof Coatings on Solar Panel Performance

4.1 Introduction

Building on the analysis from the previous chapter, which explored the impact of reflective roof coatings on HVAC loads in buildings equipped with solar panels, this chapter focuses on understanding how these reflective coated roofs affect the performance of a solar panel itself. As shown in Figures 2-3 and 2-4, reflective coatings primarily aim to lower roof surface temperatures. A cooler surface underneath the solar panel is anticipated to enhance solar panel performance, given their efficiency increases in lower temperature conditions.

The operating temperature of a photovoltaic panel is a function of various factors including the ambient temperature, wind speed, PV material, solar radiation, angle of inclination. The operating temperature directly influences the efficiency with which the PV panel converts solar energy into electrical energy. The effects of operating temperatures of PV on efficiency are very well studied in the literature. [37]

4.2 Thermal model for a photovoltaic module

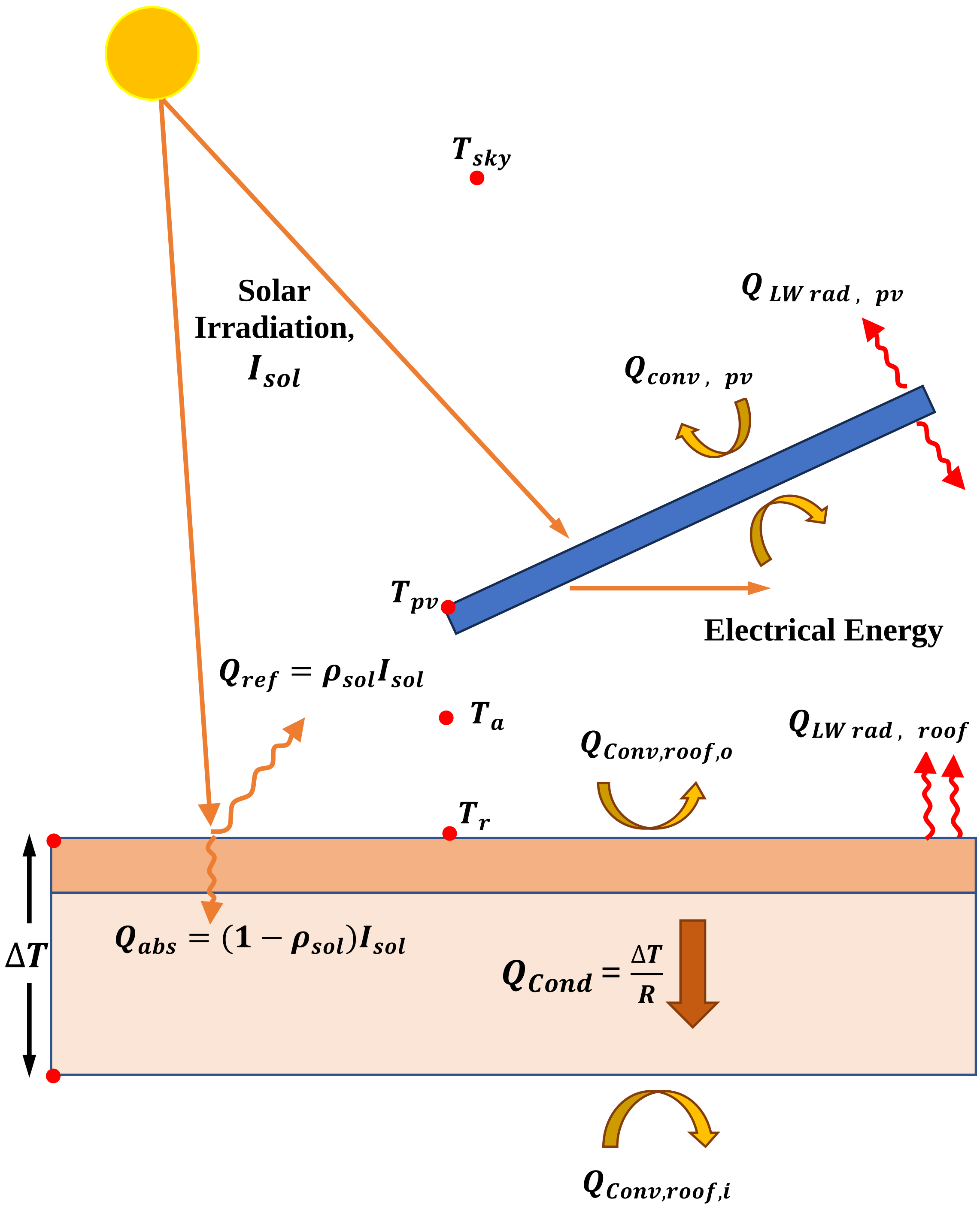

Figure 4-1: Heat Transfer Model for the PV

Figure 4-1 shows the pictorial representation of energy balance on the roof and the PV. Solar energy incident on the panel is converted into electrical energy, typically ranging from 10% to 25% in commercially available solar panels. Convection and radiation are the two modes of heat transfer with which this absorbed solar thermal energy is dissipated into the surroundings.

The fundamental principle governing the thermal modeling of a PV panel is the first law of thermodynamics. For an efficient operation, the energy absorbed from the sun must be dissipated to the surroundings in order to limit the PV temperatures. Applying the law of conservation of energy on a PV cooled by its surroundings we get,

$$Q_{solar} = E_{elec} + Q_{losses} \qquad \text{Eq – 4-1}$$

Such an equation is used by John A Duffie [38] to calculate cell temperatures. However, the analysis doesn't include the dependence of cell temperature on the roof temperatures. Several other popular models such as one developed by Faiman, 2008 [39] and Sandia (King et al, 2004) [40] also provide expressions for cell temperatures that do not factor in roof temperatures. Cell temperatures from these three models are summarized in Table 4-1.

Table 4-1: Various Models for Calculating PV Cell Temperature

Cell temperature equation	Model	Reference
$$\frac{T_c - T_a}{T_{NOCT} - T_{a,NOCT}} = \frac{G_T}{G_{NOCT}} \frac{U_{L,NOCT}}{U_L}\left[1 - \frac{\eta_c}{(\tau\alpha)}\right]$$ • T_c is module temperature (°C) • T_a is ambient air temperature (°C) • $\tau\alpha$ is effective transmittance-absorptance product • U_L is loss coefficient • The nominal operating cell temperature (NOCT) is defined as the cell or module temperature that is reached at a solar radiation level of 800 W m^{-2}, a wind speed of 1 m/s, an ambient temperature of 20°C, and no-load operation (i.e., with $\eta_c = 0$).	Duffie	[38]
$$T_m = T_a + \frac{E_{POA}}{U_0 + U_1 \times WS}$$ • T_m is module temperature (°C) • T_a is ambient air temperature (°C) • E_{POA} is the irradiance incident on the plane of the module or array (W/m^2) • U_0 is the constant heat transfer component (W/m^2K) • U_1 is the convective heat transfer component (W/m^3sK) • WS is wind speed (m/s)	Faiman	[39]
$$T_m = E_{POA} \cdot e^{a+b \cdot WS} + T_a$$ • T_m is module temperature • E_{POA} is solar irradiance incident on the module (POA) (W/m^2) • T_a is ambient air temperature (°C) • WS is Wind speed (m s^{-1}) • a and b are constant parameters that depend on the module construction and materials as well as on the mounting configuration of the module	Sandia	[40]

EnergyPlus offers various models to simulate solar panels [27, 41]. They are summarized as follows:

1. **Simple Model**:

    - The electrical power generated is given by Eq – 4-2

$$E_{generated} = AreaFraction_{pv} \ \eta_{cell} \, \eta_{invertor} \, I_s \qquad \text{Eq – 4-2}$$

    - Cannot model efficiencies based on operating conditions but allows users to specify conversion efficiencies for the cell and inverter.
    - Suitable for early design analysis without any analysis in detail.

2. **Equivalent One-Diode Model**:

    - Utilizes a four-parameter empirical approach to forecast the electrical behavior of crystalline PV modules.
    - Simulates a PV module with an equivalent circuit consisting of a direct-current source, diode, and one or two resistors.
    - Determines current as a function of load voltage and provides outputs such as current and voltage at the maximum power point, open-circuit voltage, and short-circuit current.
    - Calculates cell temperature using Duffie [38] model as given in Table 1 to determine electrical output.

3. **Sandia Model**:

- Based on research at Sandia National Laboratory, it consists of empirical relationships with coefficients derived from experimental tests.
- Calculates five select points on the current-voltage curve, assuming module operation only at the maximum power point.
- Predicts module performance based on cell temperature given by equation [40] in Table 4-1.

None of the models available in EnergyPlus are appropriate for examining the impact of reflective roof coatings on solar panel performance, as they do not consider the effect of roof surface temperatures. Consequently, EnergyPlus is not suitable for conducting such an analysis. To expand upon the literature, it is required to study the effect of reduced roof temperatures resulting from the application of reflective coatings on the cell temperatures. Therefore, the study aims to develop a thermal model of the PV system employing an energy balance approach. Hourly weather data and the calculated temperatures for a black roof and the reflective roof for a strip mall building in Phoenix are utilized as inputs to the model, sourced from EnergyPlus.

The losses to the environment as described by Eq – 4-3 can further be divided into convection and radiation and Eq – 4-1 can be re-written as

$$Q_{solar} = E_{elec} + Q_{LW\,rad,\ pv} + \ Q_{conv,\ pv} \qquad \text{Eq – 4-3}$$

where

Q_{solar} is solar energy absorbed by the solar panel

E_{elec} is output in form of electrical energy

$Q_{conv,\ pv}$ is the heat dissipated to the surrounding air in the form of convection

$Q_{LW\,rad,\ pv}$ is the heat loss in the form of long-wave radiation

Solar radiation:

The net solar radiation absorbed by the panel is a function of several factors including solar irradiation, the area of the panel, transmissivity of the glass and the solar absorptivity of the PV material. This relationship is mathematically expressed by Eq – 4-4. Often, an anti-reflective coating is applied over the panels to enhance the solar absorptance value.

$$Q_{solar} = (\tau\alpha)\, I_s\, A_{pv} \qquad \text{Eq – 4-4}$$

where,

τ is Trasmissivity of PV glass

α is solar absorptance of PV cell

I_s is incident solar irradiation (W/m^2)

A_{pv} is area of the module (m^2)

Electrical Energy:

The power output generated by the PV panel depends on solar irradiation and the efficiency of the panel. Several researchers have evaluated the efficiency of panels as a function of operating temperatures [37]. In this study, the following relationship as given by Eq – 4-5 is employed to compute the power output from the panel. [42, 43]

$$E_{electrical} = A_{pv}\, \eta_{T_{ref}} \left(1 + \beta_{ref}\, (T_{pv} - T_{ref})\right) I_s \qquad \text{Eq – 4-5}$$

where,

$\eta_{T_{ref}}$ represents efficiency at a reference temperature of 25ºC and an irradiance of 1000 W/m^2

T_{ref} is reference temperature of 25ºC

β_{ref} denotes the temperature coefficient, equal to -0.004/ºC

Convective heat transfer

As given by Newton's law of cooling, the convective heat transfer between the PV module surface and the surrounding air depends on the convective heat transfer coefficient and temperature difference between them. For a PV interacting with ambient air, this can be expressed as follows:

$$Q_{convection} = A_{pv}\, h_{conv}\left(T_{pv} - T_{air}\right) \quad \text{Eq – 4-6}$$

where,

h_{conv} the denotes convection heat transfer coefficient

T_{pv} is the temperature of PV module

T_{air} is temperature of ambient air

Figure 4-2 [44] summarizes the research [44, 45,46,47,48] done in the past that aimed to experimentally evaluate the convective heat transfer coefficient between the PV panel and the surrounding air. In this study, the approach used by W. Hu, X. Li, J. Wang et al. [44] is used, considering its incorporation of the panel's tilt angle. The convective heat transfer coefficient as a function of wind speed [44] can be represented by Eq–4-7:

$$h_{conv} = p_1 w_{speed} + p_2 \quad \text{Eq – 4-7}$$

where p_1 and p_2 are constants and are defined as a function of tilt angle, θ, of the PV as follows:

$$p_1 = \begin{cases} -0.26 \cdot \theta + 3.65, & \theta < \frac{\pi}{4} \\ 0.85 \cdot \theta + 2.71, & \theta \geq \frac{\pi}{4} \end{cases} \qquad p_2 = \begin{cases} 2.18 \cdot \theta + 13.07, & \theta < \frac{\pi}{4} \\ 0.47 \cdot \theta + 14.39, & \theta \geq \frac{\pi}{4} \end{cases}$$

Eq – 4-8

Figure 4-2 illustrates a comparison among various models, establishing a relationship between the convective heat transfer coefficient and wind speed. Despite different conditions, all the models closely align with each other. In this study, the relationship for a tilt angle of 35 degrees will be represented by a line between the red and black dotted lines in Figure 4-2.

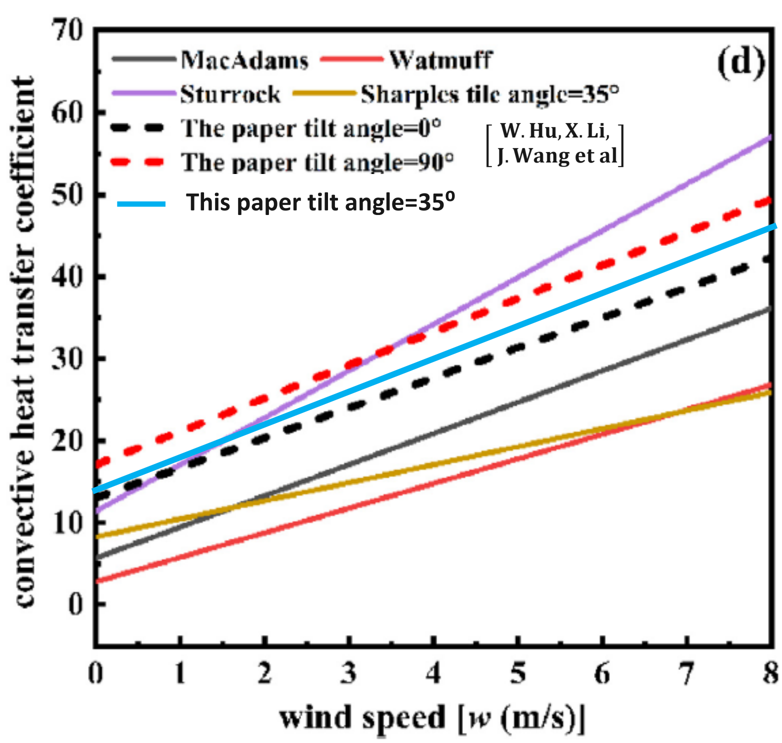

Figure 4-2: Heat transfer coefficient comparison between various models [44]

Radiation heat transfer

Radiation heat transfer involves the exchange of heat in the form of long-wavelength radiation from various surfaces. Governed by Stefan-Boltzmann's law, radiation heat exchange in a PV cell occurs between the front surface, back surface, sky, and roof, as expressed in Equations 4-9, 4-10 and 4-11 below:

$$Q_{radiation} = Q_{radiation,f} + Q_{radiation,b} \qquad \text{Eq – 4-9}$$

$$Q_{radiation,f} = \sigma A_{pv}\left[\epsilon_f F_{fs}\left(T_{pv}^4 - T_{sky}^4\right)\right] + \sigma A_{pv}\left[\epsilon_f F_{fr}\left(T_{pv}^4 - T_{roof}^4\right)\right] \qquad \text{Eq – 4-10}$$

$$Q_{radiation,b} = \sigma A_{pv}\left[\epsilon_b F_{bs}\left(T_{pv}^4 - T_{sky}^4\right)\right] + \sigma A_{pv}\left[\epsilon_b F_{br}\left(T_{pv}^4 - T_{roof}^4\right)\right] \qquad \text{Eq – 4-11}$$

In the above equations

σ is Stefan-Boltzmann constant (5.6697×10^{-8} W m^{-2} K^{-4})

T_{pv} , T_{sky} , T_{roof} are the temperatures of PV module, sky and roof, respectively.

$\epsilon_f, and\ \epsilon_b$ represent the emissivity of the front and back surfaces of PV respectively.

F_{fs}, F_{fr}, F_{bs}, F_{br} are view factors between front surface-sky, front surface-roof, back surface-sky, back surface-roof respectively, calculated as a function of tilt angle, θ of PV panel as follows [49, 50]:

$$F_{fs} = \frac{1}{2}(1 + \cos\theta) \qquad F_{fr} = \frac{1}{2}(1 - \cos\theta)$$

$$F_{bs} = \frac{1}{2}(1 + \cos(180 - \theta)) \qquad F_{br} = \frac{1}{2}(1 - \cos(180 - \theta))$$

Eq – 4-12

Sky temperatures are determined using the EnergyPlus sky modeling approach [27], with effective mean sky temperature, T_{sky} expressed as:

$$T_{sky} = \left(\frac{IRH}{\sigma}\right)^{0.25} \qquad \text{Eq – 4-13}$$

T_{sky} is effective mean sky temperature, or sky radiative temperature, in K.

IRH represents the rate of infrared radiation (W/m^2) emitted from the sky falling onto a horizontal upward-facing surface, calculated using Eq – 4-14:

$$IRH = \sigma\, T_{sky}^4 = \epsilon_{sky}\, \sigma\, T_{air}^4 \qquad \text{Eq – 4-14}$$

where:

T_{air} is the dry-bulb temperature of ambient air

ϵ_{sky} denotes the emissivity of sky. For a clear sky, it is determined using Clark & Allen [51] correlation as follows:

$$\epsilon_{clear\ sky} = 0.787 + 0.764\left(\log\frac{T_{dp}}{273}\right) \qquad \text{Eq – 4-15}$$

T_{dp} is the dewpoint temperature, in K

In cases where the sky is covered with opaque clouds, the emissivity can be determined using the following relation from Walton (1983) [52]:

$$\epsilon_{sky} = \epsilon_{clear\ sky}(1 + 0.0224N - 0.0035N^2 + 0.00028N^3) \qquad \text{Eq – 4-16}$$

N represents opaque sky cover expressed in tenths

This formula provides a means to adjust the emissivity of the sky based on the extent of cloud cover. In this study, there is no consideration for opaque cloud cover, assuming clear skies throughout.

PV Energy Balance Equation:

The PV energy balance equation can be derived by substituting expressions from Eq – 4-4, Eq – 4-5, Eq – 4-6 and Eq – 4-9 into Eq – 4-1, resulting in the final equation incorporating all relevant parameters:

$$\tau\alpha\, I_s\, A_{pv} - A_{pv}\, \eta_{T_{ref}} \left(1 + \beta_{ref}\left(T_{pv} - T_{ref}\right)\right) I_s - A_{pv}\, h_{conv}\left(T_{pv} - T_{air}\right)$$
$$- \Big[\sigma A_{pv}\left[\epsilon_f F_{fs}\left(T_{pv}^4 - T_{sky}^4\right)\right] + \sigma A_{pv}\left[\epsilon_f F_{fr}\left(T_{pv}^4 - T_{roof}^4\right)\right]$$
$$+ \sigma A_{pv}\left[\epsilon_b F_{bs}\left(T_{pv}^4 - T_{sky}^4\right)\right] + \sigma A_{pv}\left[\epsilon_b F_{br}\left(T_{pv}^4 - T_{roof}^4\right)\right]\Big] = 0$$

Eq – 4-17

Note that the above equation represents a steady-state energy balance equation. Studies have indicated that steady-state models provide reasonably accurate results when weather data is averaged over longer time intervals, typically greater than hourly [53]. Hourly data, which is usually obtained by averaging weather data recorded at shorter intervals (typically every minute), assumes constant environmental conditions (such as irradiance, temperature, and wind speed) within the hourly intervals. The steady-state assumption is considered a good approximation when weather conditions remain stable within each hour. However, it's important to acknowledge that averaging weather data to longer time intervals may result in an overestimation of power output of the solar panel, as extreme weather data values are smoothed out during averaging [53]. For crystalline silicon modules, this overestimation could be on the order of 1% when using hourly time intervals [53]. Research has shown that transient thermal models for PV modules can improve model accuracy by approximately 0.58% compared to steady-state models [54]. In this study, the weather data is averaged at hourly intervals, making steady-state conditions a reasonable assumption for calculating module temperatures. Furthermore, since the study compares a black roof to a coated roof, any overestimation in both cases is not expected to significantly affect the percentage change. The slightly reduced accuracy of the steady-state model compared to the transient model is unlikely to have a substantial impact as long as the comparison between the black roof and coated roof is made under identical environmental conditions for both roofs. A similar kind of equation is the basis for Duffie's widely used NOCT model [38] in which convection and radiation are combinedly governed by single loss coefficient (Table 4-1). The NOCT model for calculating cell temperatures is widely used in various PV modelling software such as SAM, EnergyPlus and PVsyst. Since Eq – 4-17 evaluates the effects of convection and radiation separately, it is possible to show the dependence of cell temperatures on roof temperatures. The above equation was solved using the parameter values listed in Table 4-2 to obtain hourly module temperature values for both a black roof (SR=0.05, TE=0.9) and a coated roof (SR=0.84, TE=0.9) in Phoenix, Arizona. Roof temperature values were calculated using EnergyPlus for a strip-mall building (2090.32 m^2) with solar panels covering 75% of the roof area. Other parameters such as the convective heat transfer coefficient and sky temperature were derived from hourly solar irradiance, ambient dry bulb temperature, dew point temperature, and wind speed data obtained from the EnergyPlus weather file.

Table 4-2: Parameters to Solve PV Equation

Parameter	Value
Transmittance-absorptance product, $\tau\alpha$	0.9
Temperature coefficient, β_{ref}	-0.004/C
Reference Temperature, T_{ref}	25ºC
Efficiency at reference temperature of 25ºC and Irradiance of 1000 W/sqm, $\eta_{T_{ref}}$	16%
PV tilt angle, θ	32º
Area cover by PV, A_{pv}	1567.5 m^2
Emissivity, ϵ_f and ϵ_b	0.9
Solar irradiance, I_s (W/m^2)	Hourly values from EnergyPlus weather file for Phoenix, AZ
Ambient dry bulb temperature, T_{air} (ºC)	Hourly values from EnergyPlus weather file for Phoenix, AZ
Roof temperature, T_{roof}	Hourly values calculated using EnergyPlus with solar panel (Area Fraction = 0.75) acting as a shading surface in strip-mall building (2090.32m^2) in Phoenix, AZ

4.3 Results

Figure 4-3 shows the comparison of annual roof temperatures of a black roof and the coated roof. It can be observed that the black roof consistently maintains significantly higher temperatures compared to the coated roof. During nighttime, both roofs exhibit similar temperatures due to their identical thermal emittance values of 0.9. However, during daytime hours, the black roof can experience temperatures 20°F to 30°F higher than the coated roof for most of the year. As mentioned previously, these temperatures were obtained using EnergyPlus for a strip-mall building in Phoenix, Arizona and were utilized as an input to the PV thermal model.

In Figure 4-4, the annual PV module temperatures for both the black roof and the coated roof are shown. It can be observed that there are days where the temperature of the PV modules installed on the coated roof is more than 4°F lower compared to those installed on the black roof. As discussed earlier, the efficiency of PV module is a function of its operating temperature. Consequently, the module over the coated roof exhibits higher efficiency than the one installed on the black roof during most times of the year. The comparison of operating efficiencies for both PV modules is presented in Figure 4-5.

Using the hourly operating efficiencies, annual power is calculated using Eq – 4-5 for both the modules. The results indicate that module over the coated roof generates approximately 489,817 kWh of annual energy, which is approximately 3,707 kWh more as compared to the energy generated by the module on the black roof resulting in a 0.8% increase in annual energy generation. It is interesting to note that there is an additional potential for PV modules on the coated roof to generate more energy apart from the extra energy generated due to its improved performance. This is attributed to the increased solar irradiance falling on the solar panels after reflecting from the cool roof coatings. Previous experiments conducted by researchers have indicated higher solar irradiance on the panel after reflection from the coating [55]. Overall, the positive impact of reflecting coatings on the performance of solar panels is evident.

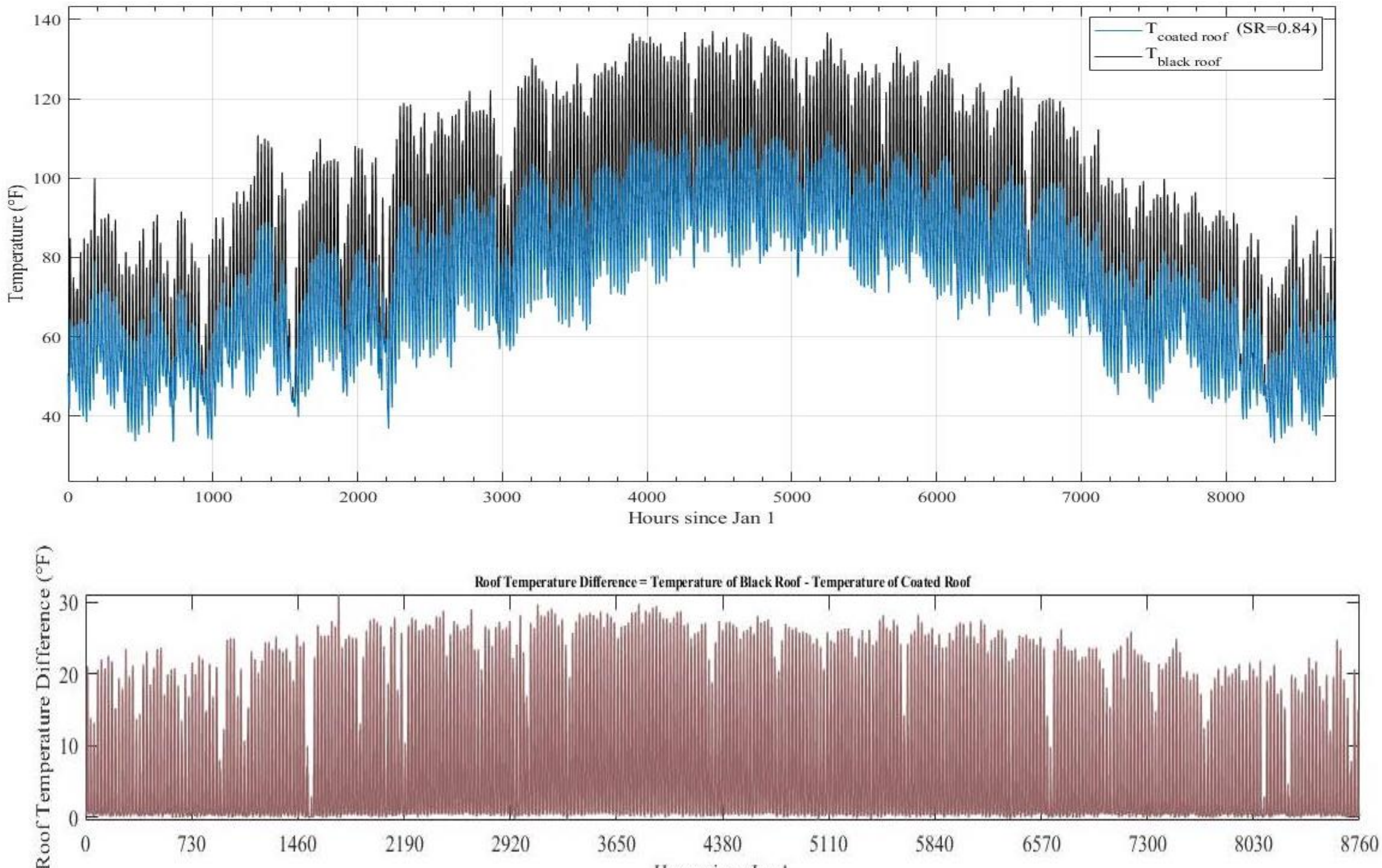

Figure 4-3: Black Roof Temperature vs Coated Roof Temperature

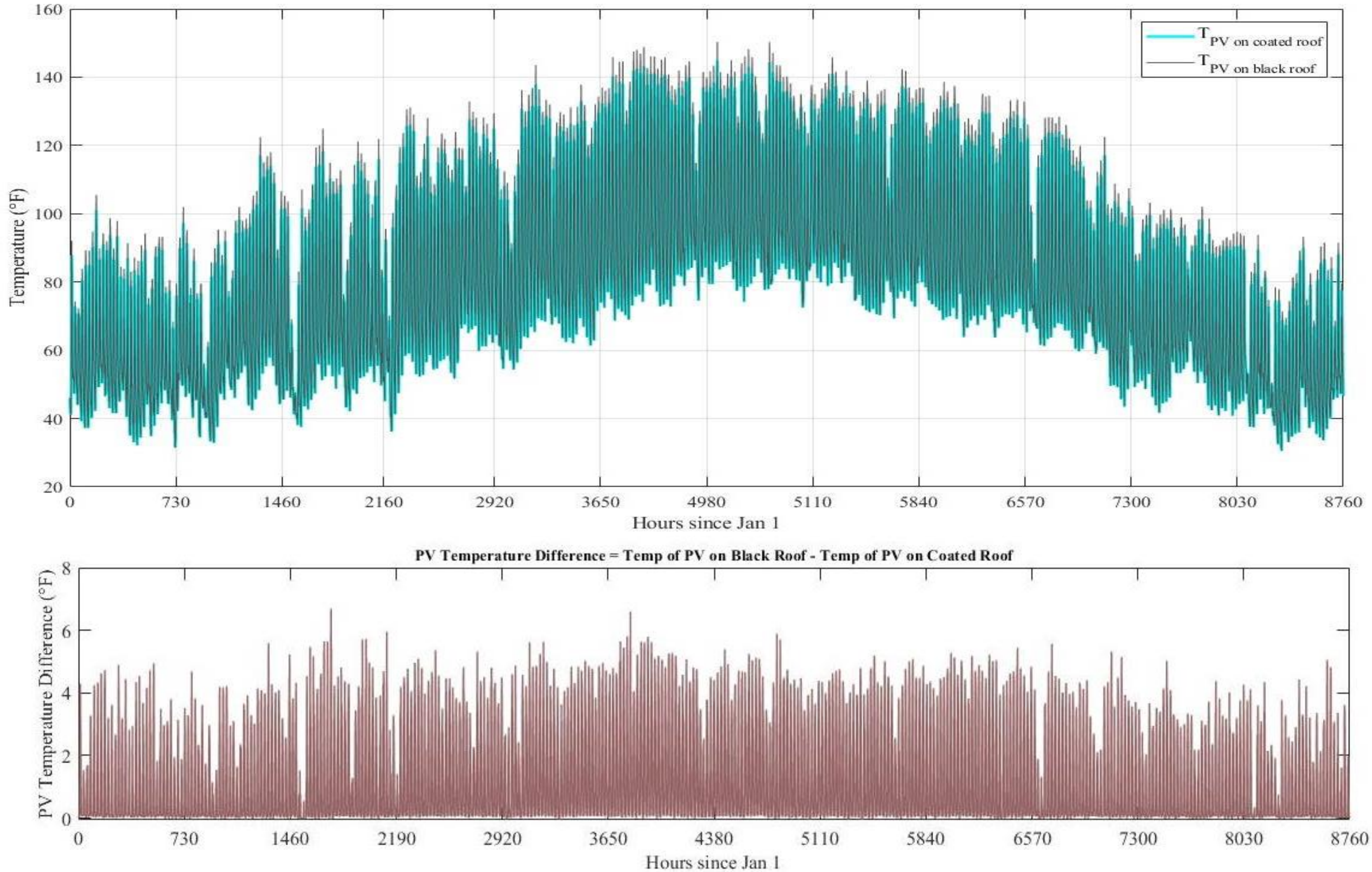

Figure 4-4: Temperature of Module on Black Roof vs Temperature of Module on Coated Roof

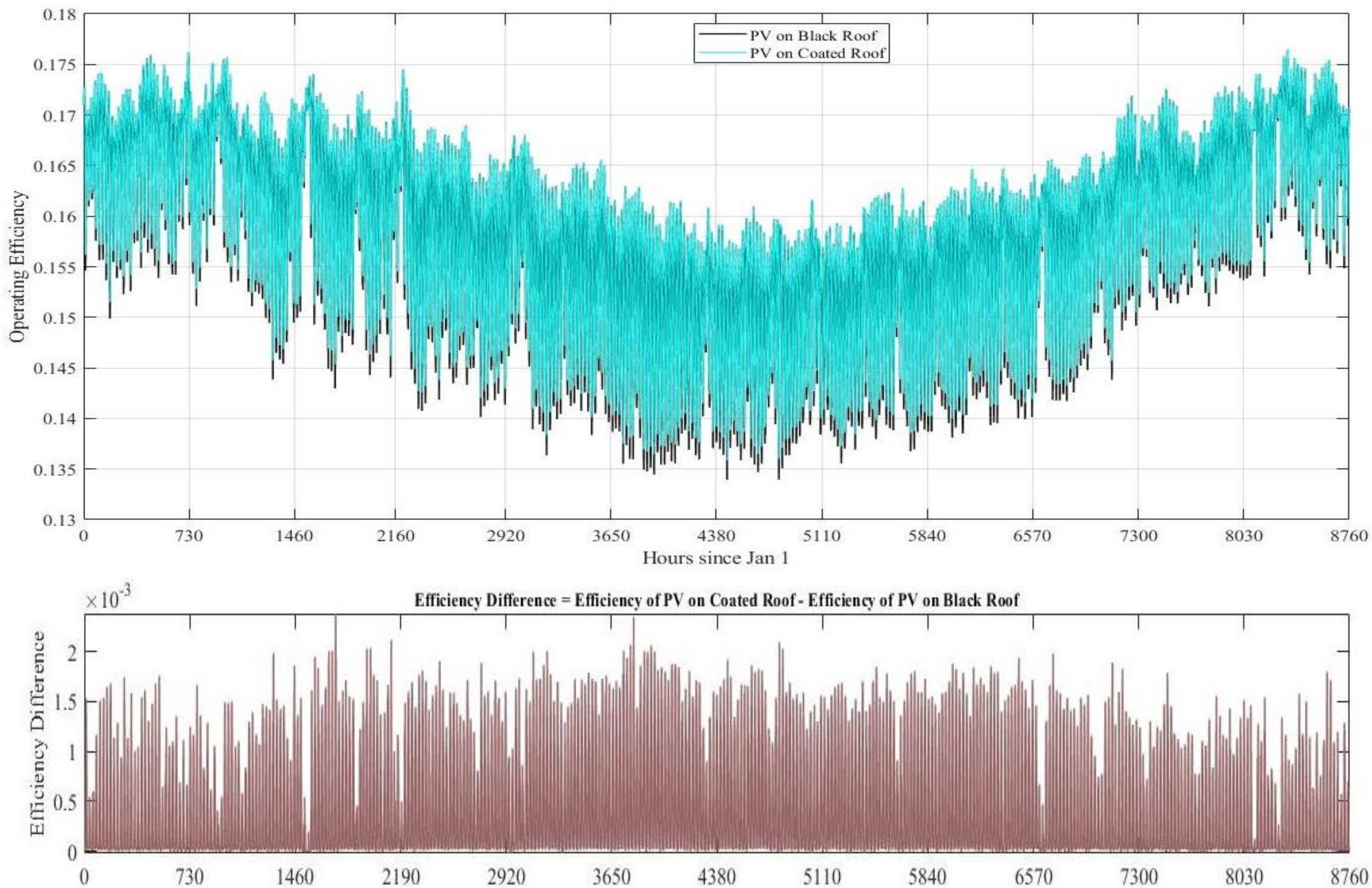

Figure 4-5: Efficiency of Module on Black Roof vs Efficiency of Module on Coated Roof

CONCLUSION

In conclusion, this work studies the role of reflective roof coatings as a passive means to save energy, not only by reducing the building HVAC loads but also by enhancing the performance of solar panels installed on rooftops. From the analysis done across four distinct climates—Phoenix, Houston, Los Angeles, and Miami—it is evident that Miami exhibits the highest energy savings with commercially available reflective roof coatings. Since coatings have the ability to lower roof surface temperatures, which is the reason behind energy savings, there is further potential for them to help mitigate the urban heat island effect in cities. The study on the effect of solar reflectance and thermal emittance values on roof surface temperatures highlights the importance of higher values of both the properties. It is also shown that solar reflectance is most influential in temperature reduction. Additionally, the study on the combined impact of thermal insulation and roof coating on building HVAC loads suggests a higher energy-saving potential in buildings with poor insulation. Lastly, the third and the fourth chapters demonstrate how the installation of photovoltaic panels with cool roof coatings on rooftops can lower the cooling demands and improve the panel efficiency as well.

REFERENCES

1. The World Bank: Urban Development https://www.worldbank.org/en/topic/urbandevelopment/overview#1

2. United Nations Population Division. World Urbanization Prospects: 2018 Revision. Available at https://population.un.org/wup/Publications/Files/WUP2018-Report.pdf

3. Donald M. Yow, (2007), Urban Heat Islands: Observations, Impacts, and Adaptation

4. Konopacki, S, Gartland, L, Akbari, H, & Rainer, L. (1998) Demonstration of energy savings of cool roofs. United States.

5. Cheikh, H. B., & Bouchair, A. (2008). Experimental studies of a passive cooling roof in hot arid areas. Journal of Renewable Energies, 11(4), 515-522.

6. Sailor, D. J. (1995). Simulated urban climate response to modifications in surface albedo and vegetative cover. Journal of Applied Meteorology and Climatology, 34(7), 1694-1704.

7. Synnefa, A., Dandou, A., Santamouris, M., Tombrou, M., & Soulakellis, N. (2008). On the use of cool materials as a heat island mitigation strategy. Journal of Applied Meteorology and Climatology, 47(11), 2846-2856.

8. Jacobson, M. Z., & Ten Hoeve, J. E. (2012). Effects of urban surfaces and white roofs on global and regional climate. Journal of climate, 25(3), 1028-1044.

9. Akbari, H. (2009). Cooling our communities. A guidebook on tree planting and light-colored surfacing.

10. Rawat, M., & Singh, R.N. (2022). A study on the comparative review of cool roof thermal performance in various regions. Energy and Built Environment, 3(3), 327-347.

11. Poulek, V., Matuška, T., Libra, M., Kachalouski, E., & Sedláček, J. (2018). Influence of increased temperature on energy production of roof integrated PV panels. Energy and Buildings, 166, 418-425.

12. Skoplaki, E., & Palyvos, J. (2009). On the temperature dependence of photovoltaic module electrical performance: A review of efficiency/power correlations. Solar Energy, 83(5), 614-624.

13. Cool Roof Rating Council: https://coolroofs.org/

14. Solar Reflectance Index: https://coolroofs.org/documents/CRRC-SRI-Document_2022-07-12.pdf

15. ASHRAE Climate Zones: https://help.iesve.com/ve2021/ashrae_climate_zones.htm?ms=BQABAAAAAAAAAAAAEAAAAAAAAAAAAAAAAAAAEAAAAAAAAAAAAAAAAAAAAAAAAAAIgIBAI&st=MA%3D%3D&sct=MTMz&mw=MjQw

16. 2021 IECC - International Energy Conservation Code

17. EnergyPlus: https://energyplus.net/

18. ASHRAE Standard 140 methodology: https://www.energy.gov/eere/buildings/articles/test-procedures-building-energy-simulation-tools

19. R&D 100 award: https://science.osti.gov/About/Honors-and-Awards/RD-100-Awards/09-25-03

20. Autodesk Revit with Insight: https://www.autodesk.com/products/insight/overview

21. Rhino: https://www.rhino3d.com/

22. Grasshopper: https://www.grasshopper3d.com/

23. Honeybee: https://www.ladybug.tools/honeybee.html

24. OpenStudio SketchUp Plug-in: https://github.com/openstudiocoalition/openstudio-sketchup-plugin/releases

25. OpenStudio: https://openstudio.net/

26. DesignBuilder: https://designbuilder.co.uk/

27. EnergyPlus Engineering Reference: https://energyplus.net/assets/nrel_custom/pdfs/pdfs_v22.1.0/EngineeringReference.pdf

28. EnergyPlus Weather Data: https://energyplus.net/weather

29. Commercial Reference Buildings, U.S. Department of Energy: https://www.energy.gov/eere/buildings/commercial-reference-buildings

30. Oak Ridge National Laboratory Cool Roof Calculator: https://web.ornl.gov/sci/buildings/tools/cool-roof/input/

31. Raman, A., Anoma, M., Zhu, L. et al. (2014) Passive radiative cooling below ambient air temperature under direct sunlight. Nature 515, 540–544.

32. Mandal, J., Fu, Y., Overvig, A. C., Jia, M., Sun, K., Shi, N. N., Zhou, H., Xiao, X., Yu, N., & Yang, Y. (2018). Hierarchically porous polymer coatings for highly efficient passive daytime radiative cooling. Science.

33. Zhai, Y., Ma, Y., David, S. N., Zhao, D., Lou, R., Tan, G., Yang, R., Yin, X. (2017). Scalable-manufactured randomized glass-polymer hybrid metamaterial for daytime radiative cooling. Science, 355(6329), 1062-1066.

34. John Hollick, (2012) "Nocturnal Radiation Cooling Tests", Energy Procedia, Volume 30, Pages 930-936

35. ASHRAE Standard 90.1: https://www.ashrae.org/technical-resources/bookstore/ansi-ashrae-ies-standard-90-1-2022-changes.

36. Planning & Development Department: Self Certification Training Energy Code: https://www.phoenix.gov/pddsite/Documents/TRT/dsd_trt_pdf_00605.pdf

37. Dubey, S., Sarvaiya, J. N., & Seshadri, B. (2013). Temperature Dependent Photovoltaic (PV) Efficiency and Its Effect on PV Production in the World – A Review. Energy Procedia, 33, 311-321.

38. Duffie, J.A. and Beckman, W.A. (2013) Solar Engineering of Thermal Processes. 4th Edition, John Wiley & Sons, New York.

39. Faiman, D. (2008), Assessing the outdoor operating temperature of photovoltaic modules. Progress in Photovoltaics: Research and Applications, 16(4), 307-315.

40. D. L. King, W. E. Boyson, and J. A. Kratochvil, (2004). "Photovoltaic array performance model," Sandia National Laboratories, Albuquerque, NM,USA, Tech. Rep. SAND2004-3535

41. Griffith, B T, & Ellis, P G. (2004). Photovoltaic and Solar Thermal Modeling with the EnergyPlus Calculation Engine: Preprint. United States.

42. Notton, G., Cristofari, C., Mattei, M., & Poggi, P. (2005). Modelling of a double-glass photovoltaic module using finite differences. Applied Thermal Engineering, 25(17-18), 2854-2877.

43. Evans, D. L. (1981). "Simplified method for predicting photovoltaic array output," Solar Energy, vol. 27, no. 6, pp. 555–560.

44. Hu, W., Li, X., Wang, J., Tian, Z., Zhou, B., Wu, J., Li, R., Li, W., Ma, N., Kang, J., Wang, Y., Tian, J., & Dai, J. (2022). Experimental research on the convective heat transfer coefficient of photovoltaic panel. Renewable Energy, 185, 820-826.

45. Sharples, S., & Charlesworth, P.S. (1998). Full-scale measurements of wind-induced convective heat transfer from a roof-mounted flat plate solar collector. Solar Energy, 62, 69-77.

46. McAdams, W.H. (1954). Heat Transmission. McGraw-Hill, New York.

47. Watmuff, J.H., Charters, W.W.S. and Proctor, D. (1977) Solar and Wind Induced External Coefficients for Solar Collectors. Revue Internationale d'Heliotechnique, 2, 56.

48. N.S. Sturrock, (1971). Localized Boundary-Layer Heat Transfer from External Building Surfaces, University of Liverpool.

49. Liu, B.Y., & Jordan, R.C. (1963). The long-term average performance of flat-plate solar-energy collectors. Solar Energy, 7, 53-74.

50. Holman, J.P. (2009) Heat Transfer. 10th Edition, McGraw-Hill, New York.

51. Clark G and Allen C. (1978) The estimation of atmospheric radiation for clear and cloudy skies. Proceedings 2nd National Passive Solar Conference (AS/ISES); 675-678

52. Walton, G. N. (1983). Thermal Analysis Research Program Reference Manual. NBSSIR 83-2655. National Bureau of Standards, p. 21.

53. Hansen, Clifford & Stein, Joshua & Riley, Daniel. (2012). Effect of Time Scale on Analysis of PV System Performance. 10.13140/2.1.1150.3368.

54. Prilliman, M., Stein, J. S., Riley, D., & Tamizhmani, G. (2020). Transient Weighted Moving-Average Model of Photovoltaic Module Back-Surface Temperature. IEEE Journal of Photovoltaics, 10(4), 1053-1060.

55. Hasim Altan, Zahraa Alshikh, Vittorino Belpoliti, Young Ki Kim, Zafar Said, Monadhil Al-chaderchi. (2019). An experimental study of the impact of cool roof on solar PV electricity generations on building rooftops in Sharjah, UAE. International Journal of Low-Carbon Technologies, Volume 14, Issue 2, Pages 267–276.